Reaction valleys: mechanism of interaction of complex nuclei studied on the basis of the two-center shell model[1)]

Raj K. Gupta[2)]

Institut für Theoretische Physik der Johann Wolfgang Goethe Universität, Frankfurt am Main, Germany
Fiz. Élem. Chastits At. Yadra, 8, 717–768 (July–August 1977)

The two-center shell model and its application to nuclear fission and heavy-ion collisions is briefly reviewed. Then, in the theory of fragmentation, the asymmetric two-center shell model is generalized by the introduction of two new dynamical collective coordinates of mass and charge asymmetry. The results are given of calculations of the mass and charge distributions of fission fragments, and a study is made of the mechanisms of formation of a compound nucleus, fusion-fission reactions, and quasifission in heavy-ion collisions.

PACS numbers: 24.75.+i, 25.85.Ge, 25.70.Fg

INTRODUCTION

In this paper, the results so far obtained by means of the two-center shell model and its application to nuclear fission and heavy-ion collisions are reviewed. This model was developed because the ordinary one-center shell models encountered certain difficulties in the attempt to explain fission. By one-center models, we mean shell models with infinite oscillator potential (Nilsson model)[1] and finite-depth potentials (Woods–Saxon potential).[2–4] For description of fission at large deformations, an oscillator potential of Nilsson type becomes inapplicable as one approaches the region of separation of configurations. Indeed, this model leads to equipotential surfaces of a long, elongated, and cigar-like shape such as is shown in Fig. 1. Although potentials with finite depth are more realistic, they encounter difficulties in application due to the presence of states in the continuum and uncertainty in the choice of parameters[3] (see Sec. 2). It is intuitively clear that for nuclei whose shape undergoes large deformations and goes through the stage of formation of a neck it is more realistic to use models of potentials with two (or more) centers. A two-center oscillator model of this kind is shown in Fig. 2. Obviously, the two-center shell model gives the interesting possibility of a smooth transition from the ground states of nuclei in the Nilsson model to strongly deformed fission states and then the separate fragments.

The simplest version of a two-center oscillator can be found in Merzbacher's papers,[5] but the applications of this model to problems of nuclear physics were first made by Cherdantsev and Marshalkin[6] and Demeur and Reidemeister.[7] However, a tractable two-center shell model was in practice first solved in the work of the Frankfurt school[8–14] and was then used by many other groups.[15–26] This model is described briefly in Sec. 1.

The first successful applications of the two-center shell model to fission were made by Mosel and Schmitt[15–17] and then by Mustafa, Mosel, and Schmitt,[18] who calculated the potential energy surfaces for various fissioning nuclei. The calculations were made on the basis of Strutinskii's method of shell corrections,[27] which is set forth in Sec. 2. These investigations clearly demonstrated the advantage of the two-center shell model, which, in contrast to the one-center model, enables one to calculate the potential energy surfaces of the ground state of the compound nucleus right up to the point of separation of the fission fragments. Later, the two-center shell model was also used to calculate ion-ion potentials (potentials of elastic scattering), to study the formation of nuclear molecules in collisions of identical nuclei,[28–30] and in calculations of the potential energy surfaces of a pair of superheavy elements[31,32] in order to study the possible mechanism of their fission. The results of these investigations are summarized in Sec. 3.

However, a merely static approach to the problem of fission based on calculations of the potential energy surfaces cannot lead to quantitative comparison between theory and experiment for, as an example, the distributions of the yields of reaction products with respect to masses and charges. For this, one must introduce,

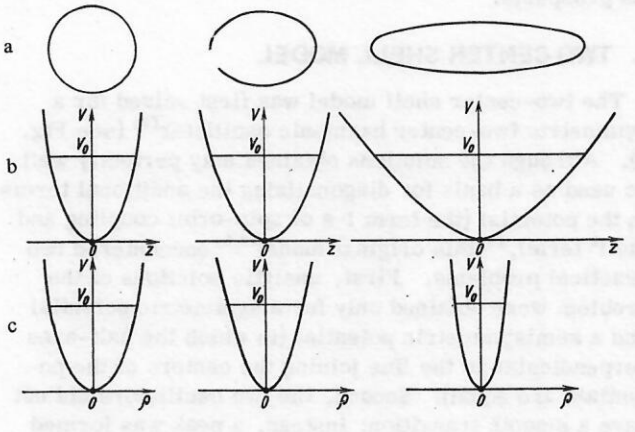

FIG. 1. Nilsson model for three values of the deformation (zero, medium, asymptotic): a) surface of the nucleus; b) potential in the z direction; c) potential in the ρ direction. V_0 is the potential that defines the surface of the nucleus.

[1)] Work supported by the Bundesministerium für Forschung und Technologie (BMFT) and by the Gesellschaft für Schwerionforschung (GSI).

[2)] Present address: Physics Faculty, Rohtak University, Rohtak (Haryana), India.

 0090-4759/77/0804-0289$02.80

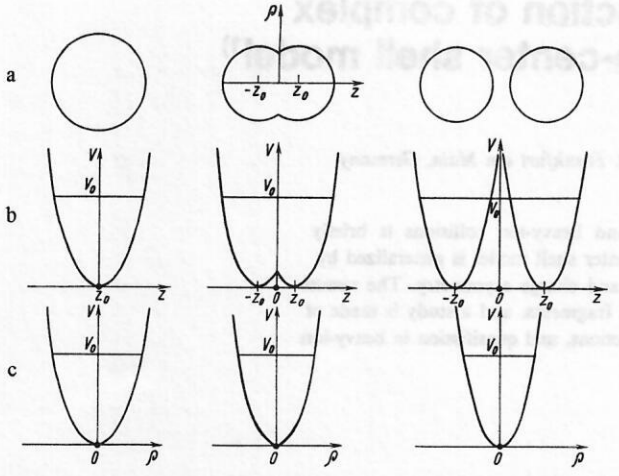

FIG. 2. Two-center oscillator model for three stages of separation of the centers (zero, medium, and asymptotic): a) surfaces of the nuclei; b) potential in the z direction; c) potential in the ρ direction.

besides the potential, the so-called mass parameters (kinetic energy) associated with the collective motion of the system. This was done in the fragmentation theory developed by generalizing the two-center shell model by the inclusion of two additional dynamical collective coordinates associated with the mass and charge fragmentation of the reaction channels.[33-47] The mass parameters are discussed in Sec. 4, and the fragmentation theory is given in Sec. 5.

The applications of fragmentation theory to nuclear fission[33-40] and heavy-ion collisions[36,38,41-46] are given Secs. 6 and 7. So far, calculations have here been made principally for the mass and charge distributions of the yields of reaction products, these explaining the basic features of the two processes.

At the present time, attempts are made to develop fragmentation theory into a completely dynamical theory. The reader can make acquaintance with the first model of such calculations in Ref. 47. The present review ends with various comments on this approach and its prospects.

1. TWO-CENTER SHELL MODEL

The two-center shell model was first solved for a symmetric two-center harmonic oscillator[8] (see Fig. 2). Although the solutions obtained may perfectly well be used as a basis for diagonalizing the additional terms in the potential (the term $\mathbf{l}\cdot\mathbf{s}$ of spin-orbit coupling and the $\mathbf{l}^2$ term),[9] this original model[8,9] encountered two practical problems. First, analytic solutions of the problem were obtained only for a symmetric potential and a semisymmetric potential (in which the half-axes perpendicular to the line joining the centers of the potentials are equal). Second, the two oscillators did not have a smooth transition; instead, a peak was formed at the position in the potential where its two fragments touched. These problems have now been overcome in the more practical asymmetric two-center shell model.[12,13,18] Other, earlier methods of solution proposed by Wong[19] and also Adeev *et al.*[21] destroy the property of incompressibility of nuclear matter; in Ref. 20, Anderson *et al.* employ a less widely used potential predicted by Nix's liquid drop model.[3] As a variant of this last method, Albrecht[25] uses the potential from Lawrence's liquid drop model.[48] Since the ideas of the transition from the one-center to the two-center shell model can be studied better in the symmetric two-center shell model, we shall consider this early variant[8-11] briefly, and then the improved asymmetric two-center shell model of Maruhn and Greiner.[13] This asymmetric model is identical with the one developed by Mustafa *et al.*[18]

Recently, in Ref. 49, Ong and Scheid proposed a method of solution for a two-center oscillator potential with finite depth that may be helpful in the future when a more realistic (Woods–Saxon) two-center potential is used.

Symmetric Two-Center Shell Model. The Hamiltonian for motion of a particle in a two-center oscillator potential in cylindrical coordinates has the form[8-11]

$$H=-(\hbar^2/2m_0)\nabla^2+[m_0\omega_0^2(z_0)/2][\rho^2+(|z|-z_0)^2]+V(\mathrm{l},\mathrm{s}). \qquad (1)$$

The first part of the potential $V(\rho,z)$ consists of two harmonic oscillator potentials with centers at the points $z=\pm z_0$ (see Fig. 2), while the second term $V(1, s)$ depends on the angular momentum and has the form

$$V(\mathrm{l},\mathrm{s})=-k\hbar\omega_0(z_0)\begin{cases}(2\mathrm{l}_1\cdot\mathrm{s}+\mu[\mathrm{l}_1^2-N(N+3)/2]), & z\leqslant 0;\\ (2\mathrm{l}_2\cdot\mathrm{s}+\mu[\mathrm{l}_2^2-N(N+3)/2]), & z\geqslant 0.\end{cases} \qquad (2)$$

Here, $\mathbf{l}_1$ and $\mathbf{l}_2$ are the angular momenta of the particle with respect to the centers $z=-z_0$ and $z=z_0$, respectively. The distance $\Delta z=2z_0$ between the two centers can be equated to the relative distance between the two nuclei and is, therefore, a very important coordinate in fission and collision problems. It follows from Eqs. (1) and (2) that for $z_0=0$ a transition takes place to the spherical Nilsson model, and that at large distances z_0 between the fragments (greater than the fragment radii) two identical and well separated potentials of the same type are formed.

Such a transition from a composite spherical system ($z_0=0$) to two separate spherical nuclei is shown in Fig. 2, and the single-particle level spectrum corresponding to this transition is given in Fig. 3. It can be seen that the calculations reproduce the shell models of the original nucleus A and the two identical fragments $A/2$, and that the level scheme for small distances between the fragments ($z_0 \lesssim 2$ F) remains of the Nilsson type. Note that the details of the spectrum depend on the method used to satisfy the condition of volume conservation, although it has been shown that the potential energy surfaces calculated by Strutinskiĭ's procedure (see Sec. 2) hardly change when these conditions are chosen in a special way.[10,11] More details of this model can be found in Refs. 8–11.

Asymmetric two-center shell model. This generalizes the symmetric model to the case when the frag-

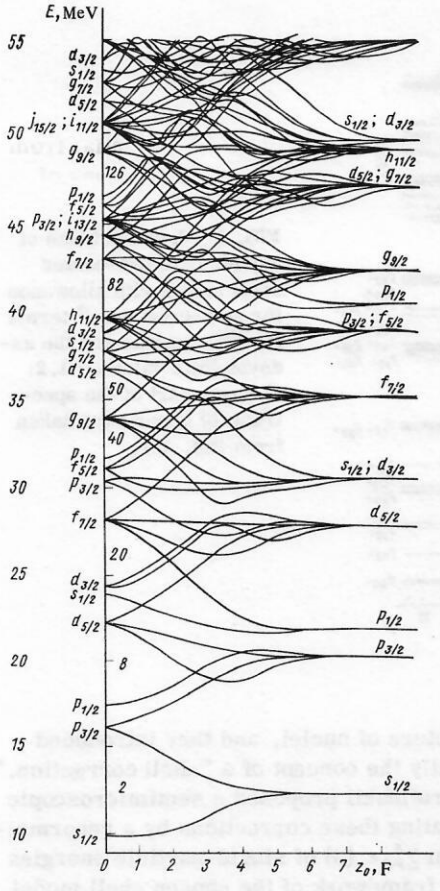

FIG. 3. Level scheme of symmetric two-center shell model with spin–orbit and l^2 terms for ^{236}U (neutrons) (Ref. 11).

ments have different deformations, and it takes into account the rounding of the barrier between the two potentials. The potential and the shape of the nucleus associated with it are given in Fig. 4 and are characterized by the following "natural" parameters[13]:

1) the distance $\Delta z = z_1 - z_2$ between the fragments. As noted above, this degree of freedom is the one most directly related to fission and collision processes;

2) the deformation parameters of the two fragments, which for the case of symmetry under rotation about the z axis are defined as $\beta_1 = a_1/b_1$ and $\beta_2 = a_2/b_2$ or, in terms of the oscillator frequencies, $\beta_1 = \omega_{\rho_1}/\omega_{z_1}$ and $\beta_2 = \omega_{\rho_2}/\omega_{z_2}$;

3) the necking-in parameter ε, defined as

$$\varepsilon = E_0/E', \tag{3}$$

where E_0 is the actual height of the barrier; E' is the height of the barrier of the two-center oscillator potential:

$$E' = m_0\omega^2 z_0^2/2 = m_0\omega_{z_1}^2 z_1^2/2 = m_0\omega_{z_2}^2 z_2^2/2. \tag{4}$$

This relation means that the barrier has the same position on the z axis as in the two-center oscillator;

4) the asymmetry parameter

$$Q = \omega_{\rho_2}/\omega_{\rho_1} = \beta_2\omega_{z_2}/\beta_1\omega_{z_1}, \tag{5}$$

which is not directly related to the mass ratio of the fragments except for the case of zero distance between the fragments and the case when the separated fragments have purely ellipsoidal shape with ratio of masses (volumes)

$$v_1/v_2 = a_1b_1^2/a_2b_2^2 = (\beta_1/\beta_2)\,Q^3. \tag{6}$$

In this limit, Q is directly related to the fundamental coordinate of fragmentation theory that characterizes the distribution of the mass of the nucleus between the fragments (see Sec. 5).

The potential of the asymmetric two-center shell model has the form

$$V(\rho, z) = \begin{cases} m_0\omega_{z_1}^2(z'^2 + \beta_1^2\rho^2)/2, & z < z_1; \\ f_0 m_0\omega_{z_i}^2 z'^2(1 + c_i z' + d_i z'^2)/2 + m_0\omega_{z_i}^2\beta_i^2\rho^2(1 + g_i z'^2)/2, \\ i = 1 \text{ and } 2;\ z_1 < z < 0;\ 0 < z < z_2; \\ m_0\omega_{z_2}^2(z'^2 + \beta_2^2\rho^2)/2, & z > z_2, \end{cases} \tag{7}$$

where

$$z' = \begin{cases} z - z_1, & z < 0; \\ z - z_2, & z > 0. \end{cases}$$

The coefficients g_1 and g_2 are introduced to avoid the appearance of peaks in the potential, and are determined by the requirement that the potential and its derivatives be continuous with respect to z at $z = 0$. This requirement gives Eq. (4) and

$$g_1 = (1 - Q^2)/(z_1\Delta z) \text{ and } g_2 = (1 - Q^2)/(z_2\Delta z Q^2). \tag{8}$$

The factor $f_0(1 + cz' + dz'^2)$ takes into account the dependence of the barrier height on the necking-in parameter ε. The dependence of the oscillator frequencies ω on the relative distance Δz between the fragments is determined numerically from the condition of volume conservation. This condition means that the surface of the nucleus is an equipotential surface of the potential, this surface bounding the same volume during each stage of the separation of the fragments.[10]

For practical calculations, it is necessary to add

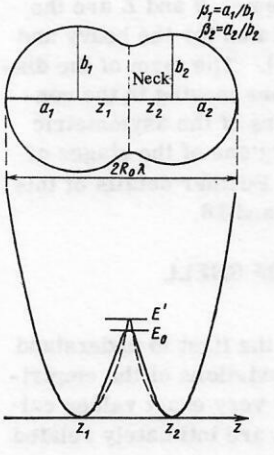

FIG. 4. Shape of asymmetric two-center potential along z axis and parameters of the model.

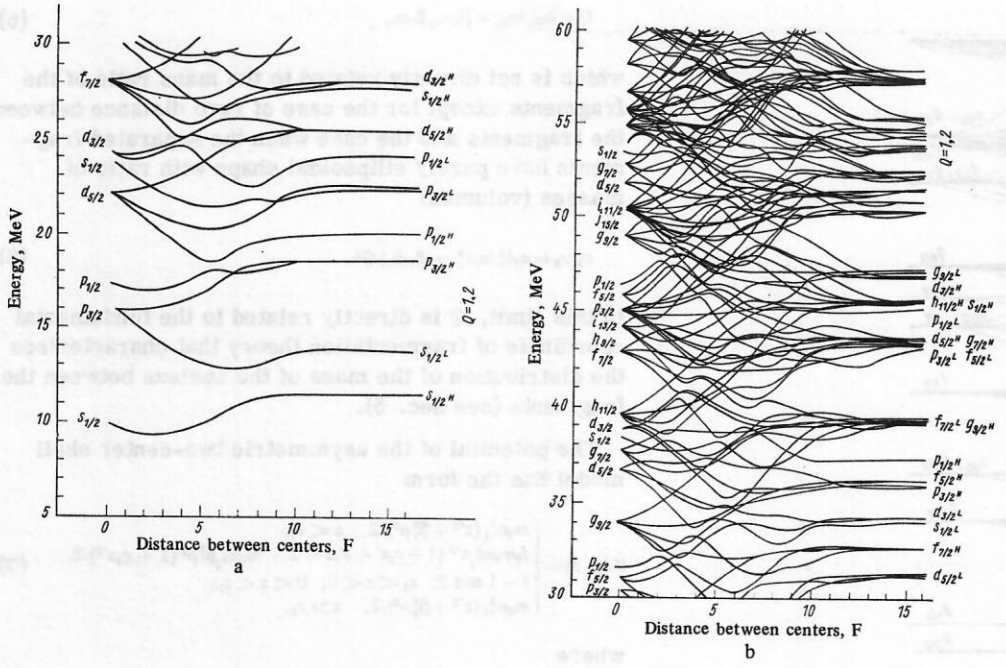

FIG. 5. Level scheme of asymmetric two-center shell model with allowance for spin-orbit and l^2 terms for ^{238}U nucleus and the asymptotic value $Q=1.2$: a) lower part of the spectrum; b) upper part (taken from Ref. 13).

$\mathbf{l}\cdot\mathbf{s}$ and l^2 terms, so that the total Hamiltonian of the model becomes

$$H=(-\hbar^2/2m_0)\nabla^2+V(\rho, z)+V(\mathrm{l}, \mathrm{s}). \quad (9)$$

The eigenvalues of this Hamiltonian are found by diagonalization in the basis of states that are completely analytic solutions of the Schrödinger equation with the potential (7) for the special case $c_i=d_i=0$ and $\beta_1\omega_{z_1}=\beta_2\omega_{z_2}$ (the last is equivalent to $Q=1$ and $g_i=0$).

The frequency ω_ρ was chosen empirically as the smallest of the values of ω_{ρ_1} and ω_{ρ_2}. The level scheme of the one-particle states obtained as a result of the calculations is shown in Fig. 5 as a function of the distance between the centers for the nucleus ^{238}U. For the asymmetry parameter Q, the following dependence on Δz was chosen: $Q=1+0.02\Delta z$ for $\Delta z<10$ F and $Q=1.2$ for $\Delta z\geq 10$ F. The asymptotic value $Q=1.2$ corresponds to fragments with masses 151 and 87. It can be seen from Fig. 5 that the level scheme reproduces the limiting cases of an initial spherical oscillator for $\Delta z=0$ and separation of it into two separate spherical oscillators corresponding to a heavy and a light fragment (in the level scheme, H and L are the indices of the single-particle states for the heavy and a light fragments, respectively). The form of the distributions of protons and neutrons moving in the connected single-particle oscillators of the asymmetric two-center shell model[39] during one of the stages of separation is shown in Fig. 6. Further details of this model can be found in Refs. 13 and 18.

2. STRUTINSKIĬ'S METHOD OF SHELL CORRECTIONS

Myers and Swiatecki[50] were the first to understand that the small but systematic deviations of the empirical masses of nuclei from their very exact values calculated in the liquid drop model are intimately related to the shell structure of nuclei, and they introduced phenomenologically the concept of a "shell correction." Subsequently, Strutinskii proposed a semimicroscopic method of calculating these corrections by a renormalization of the sum $\sum_{\nu=1}^{A}\epsilon_\nu(\beta)$ of single-particle energies calculated in the framework of the chosen shell model (which, we may mention in passing, is incapable at large deformations of giving the correct deformation energy[51]) to the corresponding energy E_{LDM} of the liquid drop model. Thus, without introducing any new parameters, he succeeded in generalizing Myers and Swiatecki's shell corrections to the case of any deformations. Very good reviews of Strutinskii's method can be found in Refs. 2 and 52. In Ref. 52, Brack discusses a verification of the method of shell corrections by comparison with the results of calculations by the Hartree–Fock method, and he also discusses its connection with the recently developed statistical and semiclassical approaches. Here, we describe in its basic features the ordinary Strutinskiĭ procedure[27] and only touch on the new definition of the shell corrections proposed in Ref. 53.

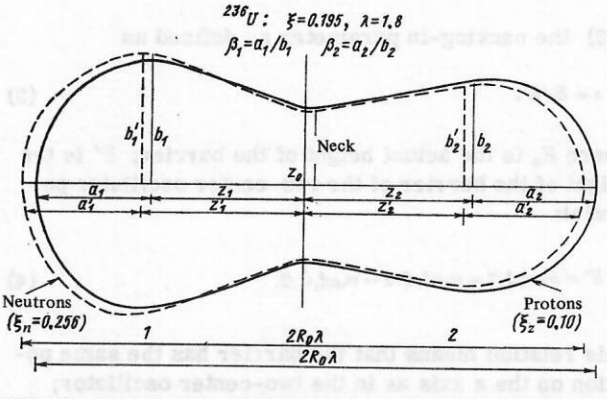

FIG. 6. Parameters of asymmetric two-center shell model for protons and neutrons (from Ref. 39).

According to Ref. 27, the shell correction δU depends on the number of nucleons A and the deformation β of the nucleus and is defined as

$$\delta U = \sum_{\nu=1}^{A} \epsilon_\nu(\beta) - \tilde{U}(A, \beta). \tag{10}$$

The smooth part $\tilde{U}$ of the energy sum can be expressed in terms of the average level density $\tilde{g}(E)$:

$$\tilde{U}(A, \beta) = \int_{-\infty}^{\lambda} E\tilde{g}(E)\, dE, \tag{11}$$

where the Fermi energy λ is determined by the condition of normalization to the number of nucleons:

$$A = \int_{-\infty}^{\lambda} \tilde{g}(E)\, dE. \tag{12}$$

In its turn, the average level density $\tilde{g}(E)$ is found by energy averaging of the single-particle spectrum ϵ_i with a Gaussian function

$$\tilde{g}(E) = \frac{1}{\sqrt{\pi}\gamma} \sum_{\nu} \exp\left[-\left(\frac{E-\epsilon_\nu}{\gamma}\right)^2\right] P_M\left(\frac{E-\epsilon_\nu}{\gamma}\right). \tag{13}$$

The smoothing parameter γ is of the distance between the principal shells $\hbar\omega$, and $P_M(x)$ is a polynomial of degree M which corrects the large-scale oscillations in the level density, the so-called correcting polynomial.

This renormalization procedure recalls the allowance for the corrections to the shell-model energy from Eq. (10) due to the pairing energy. The difference between the BCS energy and the shell-model energy is the pairing energy P:

$$P = \sum_{\nu} \epsilon_\nu v_\nu^2 - \Delta^2/G - \sum_{\nu=1}^{A} \epsilon_\nu, \tag{14}$$

so that the correction for the pairing energy is

$$\delta P = P - \tilde{P}. \tag{15}$$

Here, $\tilde{P}$ is the smooth part of the pairing energy determined from the uniform distribution of the single-particle states.[27,52]

With allowance for δU and δP for the protons and neutrons, the total energy of the system is

$$E_{\text{tot}} = E_{\text{LDM}} + \sum_{p,\, n} (\delta U + \delta P). \tag{16}$$

The total correction due to the shell structure and the pairing energy is sometimes called the shell effect in the literature.

Strutinskiĭ's method was widely used to calculate the deformation energy of nuclei (potential energy surfaces) with both harmonic oscillators and finite-depth potentials used as average field. As we have already said in the introduction, the calculations with finite-depth potentials encountered difficulties due to the fact that the number of bound states above the Fermi surface is inadequate for carrying out directly the averaging procedure. In practice, it is necessary to introduce an arbitrary cutoff in the space of single-particle states.

Strutinskiĭ and Ivanyuk[53] showed that these complications arise because Strutinskiĭ's method was explicitly formulated for an infinite range of definition of oscillating functions such as the level density. It was proposed in the general case to find the smooth component by averaging over a large but finite interval by least-squares fitting. This new procedure eliminates the difficulties for finite-depth potentials and contains, in particular, the case of an infinite averaging interval. According to Ref. 53, the total energy of the system is not (16) but

$$E_{\text{tot}} = E_{\text{LSD}} + \delta U, \tag{17}$$

where E_{LSD} is the energy in the liquid drop model with parameters found by least-squares fitting to the experimental nuclear masses. This leads to a formal definition of δU which is such that its average value ov over the region of the nuclei from which E_{LSD} was determined satisfies

$$\langle \delta U \rangle_{\text{LSD}} = 0. \tag{18}$$

Essentially, the procedure of least-squares fitting means that the polynomial P_M in Eq. (13) is replaced by the new function

$$K_M(y, x) = \sum_{k=0}^{M} P_k(y) P_k(x). \tag{19}$$

The first results of calculations of the shell corrections in accordance with the new definition are very heartening and for δU differ somewhat from the values calculated by the old method.

3. CALCULATIONS OF THE POTENTIAL ENERGY SURFACES

The first calculations of the potential energy surfaces for some fissioning nuclei on the basis of the two-center shell model and the method of shell corrections were made by Anderson *et al.*[20] However, more complete calculations were made by Mosel and Schmitt,[16] who calculated the surfaces in the form of two-dimensional contours as functions of the distance Δz between the fragments and the necking-in parameter ε (see Figs. 1–11 in Ref. 16). Only mirror-symmetric shape of the fissioning nuclei was allowed in the investigations, although the two-center potential was smoothed at the neck. The generalization to the case of asymmetric fission was made by Mustafa, Mosel, and Schmitt,[18] who calculated the potential energy surfaces as a function of the mass asymmetry parameter $Q = A_1/A_2$ (the ratio of the volumes of the two fragments) for some values of the parameter ε (see Figs. 7–11, 24, and 15 in Ref. 18), and also as two-dimensional contours on the plane of the parameters ε and Q (see Figs. 2 and 12 in Ref. 18) under the condition of minimization of the energy of deformation of the frag-

ments with respect to the two remaining parameters. On the basis of these calculations of the surfaces, they predicted, in good agreement with experiment, the heights of the fission barriers (in the region of $A = 200$), fission of isomers (in heavy actinides), preferred yield of symmetric (in the case of ^{202}Pb, ^{210}Po, ^{258}Fm, and ^{264}Fm) or asymmetric (in the case of ^{236}U, ^{248}Cm, ^{252}Fm, and ^{256}Fm) fission products, and transition from asymmetric fission in the region of the second saddle point to symmetric fission in the region of scission (for ^{202}Pb and ^{210}Po). An important result of Ref. 18 used in following calculations (see Sec. 6) is the assertion that the experimentally observed mass asymmetry in fission, i. e., the asymmetry in the distribution of the mass of the fissioning nucleus between the fragments, is correlated with the calculations of the potential energy surfaces for values of the intercenter distance parameter Δz in the region of the scission point.

Calculations of the potential energy surfaces in the two-center shell model were also made for superheavy elements ($^{A}Z =)^{296}112$ and $^{298}114$ for symmetric and asymmetric fission on the basis of the argument that these elements, if they were to be obtained, must be fissile.[31,32] For the element $^{296}112$, the potential energy surfaces do not have a second minimum, while for element $^{298}114$ it is very shallow. Beyond the saddle point, the potential energy surfaces decrease slowly with the distance between the centers. For small distances Δz for the element $^{298}114$, asymmetric fission obtains, but with increasing distance between the fragments the symmetric form becomes preferred. In both examples, at large deformations of the fissioning nucleus (in the region of scission) the potential energy surfaces are close to those predicted by the liquid drop model. This indicates softness of the expected symmetric fission fragments.

In Ref. 29, Mosel, Thomas, and Riesenfeldt extended the calculations of the potential energy surfaces in the two-center shell model to heavy-ion collisions. Under the assumption of adiabaticity with respect to the single-particle motion, which was determined by the shell model, they calculated the elastic scattering potentials of identical nuclei: $^{12}C + ^{12}C$, $^{16}O + ^{16}O$, and $^{18}O + ^{18}O$. Since the two-center shell model contains naturally a structure of molecular type for fissioning nuclei, it was expected that application of it to this problem would be helpful. It is interesting to note that, in agreement with optical-model potentials deduced from scattering experiments,[55] the calculations for the system $^{16}O + ^{16}O$ gave a relatively shallow potential. Morović and Greiner[30] constructed these potentials for a large number of systems from $^{12}C + ^{12}C$ to $^{238}U + ^{238}U$. The calculations were made both in the impulse approximation and in the adiabatic approximation with respect to the collective degrees of freedom (deformation parameters), and for the case of the impulse approximation the compression energy term was included in the liquid drop model. Systematic investigation of the potentials in the impulse approximation showed that the potential minimal responsible for the formation of the nuclear molecules is fairly deep even when very heavy ions are scattered. The minimum begins to disappear in the region of the nuclei Nd or Dy. In the adiabatic approximation, it is necessary to know the complete potential energy surfaces, and calculations of them for some systems confirm the general results obtained for potentials in the impulse approximation. As yet, it is not clear which of these approximations corresponds to the real reaction mechanism. It may be that the truth lies between them, probably closer to the adiabatic case.

In conclusion, it should be pointed out that the potential energy surfaces calculated by means of (16) are valid only approximately. Since this energy contains the kinetic energy of the collective degrees of freedom, one must subtract from it the kinetic energies of the centers of mass of the collective degrees of freedom. One must take into account similarly the accuracy for the potential energy of the centers of mass of fragments due to the description of the collective modes by means of the coordinate Δz_0. The contribution of this energy to the optential energy surfaces of the two-center shell model was recently estimated by Reinhard.[56] For motion of the center of mass of the system as a whole (in the x, y, and z directions) the contribution of the kinetic energy of the centers of the fragments is negligibly small, whereas it grows appreciably for the rotational (around the x and y axes) and vibrational (with respect to Δz_0) degrees of freedom (about 4.5 MeV in the heaviest nuclei and 9 MeV in the lightest) and depends strongly on the change in the pairing structure. The contribution of the potential energy of the centers of the fragments is very small (~0.2 MeV) for heavy nuclei but increase considerably (~2 MeV) for the lightest nuclei. Thus, according to these estimates, the calculations of the potential energy surfaces for fission and for collision of heavy ions can be regarded as fairly accurate.

4. MASS PARAMETERS

Here, we shall briefly discuss the calculation of the mass parameters. At the present time, the most practical and general method for calculating the mass parameters B_{ij} is Inglis's model of forced rotation or cranking model[57] in the BCS formalism.[58] The expression for the mass parameters in the original cranking model[57] has the form

$$B_{x_i x_j} = 2\hbar^2 \sum_{n \neq 0} \langle \varphi_0 | \partial/\partial x_i | \varphi_n \rangle \langle \varphi_n | \partial/\partial x_j | \varphi_0 \rangle / (E_n - E_0), \qquad (20)$$

where $|\varphi_0\rangle$ and $|\varphi_n\rangle$ are the wave functions of the ground state and excited states of the system with energies E_0 and E_n, respectively. The expression (20) holds if the kinetic energy is a bilinear form in the velocities:

$$T = \frac{1}{2} \sum_{i,j} B_{x_i x_j} \dot{x}_i \dot{x}_j \qquad (21)$$

and is small compared with the energy of the internal motion of the nucleons (adiabatic approximation). In

Ref. 59 it is shown that if one gives up the adiabatic approximation then higher powers of the velocity occur, these being equivalent to the introduction of velocity-dependent masses. Application of this last method to practical problems opens up new possibilities for investigations in fission and heavy-ion collisions.

With allowance for the pairing interaction, Eq. (20) takes the form[58]

$$B_{x_i x_j} = 2\hbar^2 \sum_{\mu,\nu} \frac{\langle \mu \mid \partial H/\partial x_i \mid \nu \rangle \langle \nu \mid \partial H/\partial x_j \mid \mu \rangle}{(\tilde{\varepsilon}_\mu + \tilde{\varepsilon}_\nu)^3} (u_\mu v_\nu + u_\nu v_\mu)^2 + P_{ij}, \quad (22)$$

where $\tilde{\varepsilon}_\mu$ and $\tilde{\varepsilon}_\nu$ are quasiparticle energies; P_{ij} is a small correction term that takes into account the dependence of the Fermi surface and the energy gap on the deformation.[2]

Lichtner *et al.*[60] used Eq. (22) to study the coordinate dependence of the mass parameters in the symmetric two-center shell model for processes of fission and heavy-ion collisions. They showed that at large distances between the fragments the mass parameter B_{RR} of the motion of the centers of mass of the fragments tends to the reduced mass of the fragments, and the mass parameter $B_{\beta\beta}$ of the deformation coordinates tends to a constant value equal to the two mass parameters of β vibrations in the individual fragments. However, at short distances between the fragments the mass parameter B_{RR} is more than an order of magnitude greater than the reduced mass, and both B_{RR} and $B_{\beta\beta}$ fluctuate strongly.

As was first noted by Belyaev,[58] these fluctuations in B_{RR} are related to the change in the occupation probabilities v_i of the single-particle states. Beyond the scission point, the occupation probabilities become constant, the fluctuations in B_{RR} disappear, and the small smooth variation of this parameter as it tends to the reduced mass is determined by the variation of the single-particle wave functions with the deformation. As one would expect, the interference mass term $B_{R\beta}$ after the scission point, when the motions with respect to R and β become uncoupled, tends to zero. Further, in fragmentation theory, Eq. (22) is used to calculate the mass parameters by means of the asymmetric two-center shell model.

5. FRAGMENTATION THEORY

Fragmentation theory describes two-particle reactions in which the compound system decays into two particles or is formed from them. Therefore, the coordinates of the theory must be chosen in such a way that their definition in the asymptotic region can be extrapolated into the interaction region and vice versa. In principle, such extrapolation into the region of interactions (or overlapping of the fragments) would seem to be arbitrary since the quantities measured experimentally in fission processes and nuclear collisions are the cross sections, which are determined by the asymptotic behavior of the wave function. In practice, this is however not so, because during the process of fission of the nuclei the mass and charge distributions of the fission fragments are formed already before the scission of the fragments, and in a collision of nuclei the greater part of the transfer process takes place in the interaction region. We divide the nuclear system in the interaction region into two parts (fragments) 1 and 2 by means of a perpendicular plane through the region of the neck of the composite system (see Fig. 6). The exact position of this plane is not of great significance since it passes through the point at which the fragments touch at the instant when they separate. In practice, the point is taken at the neck between the fragments. This division of the interaction region presupposes that in nuclear reactions at low energies the nuclear density remains incompressible and, therefore, to describe the density distribution of the nucleus it is sufficient to specify only coordinates of the surface. We discuss here the collective coordinates chosen to describe both the nuclear system and the nucleus–nucleus system, and then, using these coordinates, we construct the Hamiltonian and describe the method by which it is estimated.

Collective Coordinates. For the consideration of only two-particle reaction channels, we introduce the following coordinates for determining the nuclear system:

1) the relative distance R between the centers of mass of the two nuclei, which in the two-center shell model is approximately equal to the distance Δz between the centers of the two potentials. The region of overlapping is characterized by the dimensionless parameter $\lambda = l/2R_0$, where $l = a_1 + a_2 + z_2 - z_1$ (see Fig. 4); R_0 is the radius of the corresponding spherical system;

2) the collective coordinates of surfaces $\alpha^{(1)}$ and $\alpha^{(2)}$ of the two nuclei (or fragments). For systems with axial symmetry around the axis joining the centers these coordinates reduce to the quadrupole deformation coordinates β_1 and β_2, respectively. In the region of overlapping, they have already been defined in Figs. 4 and 6;

3) the necking-in parameter ε, which is defined by Eq. (3). In the asymptotic limit, $\varepsilon = 1$.

In addition to these three ordinary coordinates of the asymmetric two-center shell model, the following two new coordinates are used[33-35,37,39]:

4) the fragmentation mass and charge coordinates, respectively:

$$\eta = (A_1 - A_2)/(A_1 + A_2) \text{ and } \eta_z = (Z_1 - Z_2)/(Z_1 + Z_2). \quad (23)$$

Similarly, one can define the neutron asymmetry coordinate $\eta_n = (N_1 - N_2)/(N_1 + N_2)$. However, as dynamical coordinates it is sufficient to take any two of these three since

$$\eta = (Z/A)\,\eta_z + (N/A)\,\eta_n, \quad (24)$$

where $A = A_1 + A_2$, $Z = Z_1 + Z_2$, and $N = N_1 + N_2$.

It is convenient to introduce the new coordinates (23) because η and η_z are directly related to experimental data. Indeed, in nuclear fission and heavy-ion colli-

sions one measures the yields of the reaction products and their distribution with respect to the mass and charge. In addition, the value $\eta = 0$ corresponds to the symmetric configuration (two identical fragments), and $\eta = \pm 1$ to complete fusion of the nuclei. Thus, the coordinate η describes in a unified manner fission as well as few-nucleon, many-nucleon, and cluster transfers, and incomplete or complete fusion of nuclei in heavy-ion collisions. At the same time, the coordinate η_z describes the dispersion of the charge over the fragments.

Obviously, the definition (23) is valid only in the asymptotic limit, characterized as $R \gg R_c$. Here, R_c is a certain critical distance at which the two nuclei enter into close contact with one another. In order to make the definition (23) in the interaction region ($R < R_c$), we note that the nucleon number does not then remain a good quantum number since the nucleons can belong with a definite probability to fragments 1 or 2. We define the mass asymmetry coordinate (or similarly η_z) in terms of the density ρ of the nucleus as follows:

$$\eta = \Big(\int_1 \rho\, dr_1 - \int_2 \rho\, dr_2\Big) \Big/ \int \rho\, dr = (1/A)\Big(\int \rho\, dr_1 - \int \rho\, dr_2\Big), \qquad (25)$$

where $\rho(x) = \int \Psi^*(x_1, \ldots, x_n)\hat{\rho}(x)\Psi(x_1, \ldots, x_n)\, dr_n$ is expressed in terms of the nucleon density operator in the nucleon coordinates $\hat{\rho} = \sum_{i=1}^{A} \delta(x_i - x)$; Ψ is the total internal many-particle wave function normalized to unity.

It follows from (23) and (25) that η and η_z in the asymptotic region have discrete values, and continuous values in the region of overlapping. This particular property of η and η_z of having discrete or continuous values depending on the distance R enables one to study fission and heavy-ion collisions successively along the fission or collision trajectory.

For a homogeneous density distribution of nucleons in the nucleus, the coordinates η and η_z obviously reduce to the simpler asymmetry coordinates of the volumes of the fragments ξ and ξ_z. Then

$$\eta \xrightarrow[\rho_{\text{const}}]{} \xi = \Big(\int_1 dr_1 - \int_2 dr_2\Big) \Big/ \int dr = (v_1 - v_2)/(v_1 + v_2) \qquad (26)$$

and in the same way $\eta_z \to \xi_z$. Indeed, ξ and ξ_z are purely geometrical coordinates and they can be readily calculated for every fixed shape of the nucleus in the two-center model, whereas η and η_z contain the nuclear many-particle wave functions. It is clear that the variables η and ξ are mutually dependent:

$$\left.\begin{aligned} &\eta = \eta(\xi, \xi_z, R, \alpha_i) \quad \text{or} \quad \xi = \xi(\eta, \eta_z, R, \alpha_i) \\ &\text{and} \\ &\eta_z = \eta_z(\xi, \xi_z, R, \alpha_i) \quad \text{or} \quad \xi_z = \xi_z(\eta, \eta_z, R, \alpha_i). \end{aligned}\right\} \qquad (27)$$

During the time of overlapping of the two fragment nuclei, the internal wave functions Ψ, following the variations of the potential, will have approximately the same spatial distribution as it. Therefore,

$$\eta = \xi \quad \text{for} \quad R < R_c. \qquad (28)$$

As is shown in Ref. 44, this approximation is fairly good. Since the total volume occupied by A, Z, or N is the same, we have similarly

$$\eta_z \approx \xi_z \text{ and } \eta_N \approx \xi_N \quad \text{for} \quad R < R_c. \qquad (29)$$

However, in the asymptotic region ($R \geq R_c$) the connection between η and ξ depends strongly on the procedure of occupation of the two-center single-particle states by the nucleons, for it is this that determines the distribution of the mass between the fragments. The usual procedure is that for every value of ξ (or the other collective parameters) one constructs a Slater determinant with lowest single-particle states filled right up to the Fermi surface. For completely separated potentials in the asymmetric two-center shell model, the Fermi surface coincides with the single-particle level in each well. It is only for identical fragments, because of the degeneracy of the levels in the two wells, that the Fermi level will be situated in both potentials. Such population of the single-particle states automatically leads[34,44] to a step relationship between ξ and η.

However, as we have already mentioned above, the dynamics of the fission process can be considered only up to the scission point ($R < R_c$). On the other hand, for a heavy-ion collision the use of η and η_z instead of ξ and ξ_z may lead to some appreciable effects. This question is worthy of further investigation.

Collective Hamiltonian and Estimate of it. The collective Hamiltonian depends on the coordinates R, $\alpha^{(1)}$, $\alpha^{(2)}$, η and η_z and their velocities. It can be written as

$$H = T(\mathbf{R}, \alpha, \eta, \eta_z; \dot{\mathbf{R}}, \dot{\alpha}, \dot{\eta}, \dot{\eta}_z) + V(\mathbf{R}, \alpha, \eta, \eta_z), \qquad (30)$$

where the kinetic energy term T can be expressed as follows in terms of the mass parameters B_{ij}:

$$\begin{aligned} T = {} & \tfrac{1}{2} B_{RR}\dot{R}^2 + \tfrac{1}{2} B_{\alpha\alpha}\dot{\alpha}^2 + \tfrac{1}{2} B_{\eta\eta}\dot{\eta}^2 + \tfrac{1}{2} B_{\eta_z\eta_z}\dot{\eta}_z^2 \\ & + \mathbf{B}_{R\alpha}\dot{R}\dot{\alpha} + \mathbf{B}_{R\eta}\dot{R}\dot{\eta} + \mathbf{B}_{R\eta_z}\dot{R}\dot{\eta}_z \\ & + B_{\alpha\eta}\dot{\alpha}\dot{\eta} + B_{\alpha\eta_z}\dot{\alpha}\dot{\eta}_z + B_{\eta\eta_z}\dot{\eta}\dot{\eta}_z. \end{aligned} \qquad (31)$$

The collective potential V can be found by Strutinskii's method [see Eq. (16)] by renormalizing the sum $\sum_{\nu=1}^{A} \epsilon_\nu$ of the single-particle energies $\epsilon_\nu(R, \xi, \xi_z, \varepsilon, \beta_1, \beta_2)$ of the asymmetric two-center shell model, Myers and Swiatecki's liquid drop model[50] with modified surface a symmetry constant[61] being used for this. In the interaction region ($R < R_c$), the potential is minimized with respect to ε, β_1, and β_2, which presupposes adiabaticity with respect to these coordinates. With this simplification, we avoid a dynamical investigation with respect to these coordinate. The collective energy, minimized in the $\varepsilon - \beta$ space, becomes equal to ($\eta \approx \xi$ and $\eta_z \approx \xi_z$)

$$\begin{aligned} E = {} & B_{RR}\dot{R}^2/2 + B_{\xi\xi}\dot{\xi}^2/2 + B_{\xi_z\xi_z}\dot{\xi}_z^2/2 \\ & + \mathbf{B}_{R\xi}\dot{R}\dot{\xi} + \mathbf{B}_{R\xi_z}\dot{R}\dot{\xi}_z + B_{\xi\xi_z}\dot{\xi}\dot{\xi}_z + V(\mathbf{R}, \xi, \xi_z). \end{aligned} \qquad (32)$$

The mass parameters B_{ij} are calculated in the frame-

work of the asymmetric two-center shell model by means of the cranking formula with allowance for pairing [see (22)].

In the asymptotic region ($R \geq R_c$), the potential is merely the Coulomb interaction plus the sum of the binding energies of the ground states of the two fragments:

$$V(R, \eta, \eta_z, \beta_1, \beta_2) = Z_1 Z_2 e^2/R - B(A_1, Z_1, \beta_1) - B(A_2, Z_2, \beta_2). \quad (33)$$

The binding energies $B(A_i, Z_i, \beta_i)$ are taken from Seeger's tables of atomic masses,[62] where they are given for $Z \geq 20$ with inclusion of the shell corrections calculated in the Nilsson model. Since the two-center shell model at large distances between the fragments goes over into the Nilsson model for each fragment (see Sec. 1), the potential has a continuous transition from the interaction region to the asymptotic region. The validity of this is confirmed by direct calculations[44] in accordance with the two-center model in the asymptotic region. The potential $V(R, \eta, \eta_z)$ is then found[37] by minimizing it for each possible fragmentation with respect to the mass and the charge. In other words, the potential $V(\eta_z)$ of the charge dispersion is calculated for each value of η, and in this way the minimization with respect to the coordinate β is performed automatically. Note that as $R \to \infty$ the potential V in (33) does not depend on R except through the long-range Coulomb potential, so that $V(\eta, \eta_z)$ describes the purely nuclear effects due to the difference between the structures in the different fragments. The collective energy is again given by Eq. (32) with the substitution $\xi \to \eta$ and $\xi_z \to \eta_z$.

To determine the asymptotic values of the mass parameters $B_{\eta\eta}$ and $B_{\eta_z\eta_z}$, we note that the two-center shell model is constructed using the concepts of the coordinates ξ and ξ_z. Therefore, the expression for the cranking model (22) gives the masses $B_{\xi\xi}$ and $B_{\xi_z\xi_z}$, which, using (27), one can transform into the masses of the η and η_z motions. Thus, one can write[34,36]

$$\frac{1}{2} B_{\xi\xi}\dot{\xi}^2 = \frac{1}{2} B_{\xi\xi}\left(\frac{\partial\xi}{\partial\eta}\dot{\eta} + \frac{\partial\xi}{\partial\eta_z}\dot{\eta}_z + \frac{\partial\xi}{\partial R}\dot{R} + \frac{\partial\xi}{\partial\alpha_i}\dot{\alpha}_i\right)^2. \quad (34)$$

In the first approximation, (34) gives us $\xi(\eta)$ and $\xi_z \times (\eta_z)$. For example, one can obtain

$$B_{\xi\xi}\dot{\xi}^2/2 = B_{\eta\eta}\dot{\eta}^2/2$$

together with

$$B_{\eta\eta} = B_{\xi\xi}(\partial\xi/\partial\eta)^2 \quad (35)$$

and similarly

$$B_{\eta_z\eta_z} = B_{\xi_z\xi_z}(\partial\xi_z/\partial\eta_z)^2. \quad (36)$$

Therefore, the mass parameters $\eta\eta$ and $\eta_z\eta_z$ are determined by Eqs. (27) by means of the factors $(\partial\xi/\partial\eta)^2$ and $(\partial\xi_z/\partial\eta_z)$. A check calculation was made in Ref. 44. As one expected,[60] for the region $R > R_c$ the parameter B_{RR} approaches the reduced mass of the system, and the mass parameter $B_{R\eta}$ of the coupling becomes negligibly small.

Below, we shall consider the application of this theory to fission problems (Sec. 6) and heavy-ion collisions (Sec. 7).

6. NUCLEAR FISSION

The two-center model was first applied to fission problems by Irvine and Pwu,[63] who, using the WKB approximation to calculate the barrier transmission, obtained fairly good results for the mass yields of fragments from spontaneous fission in the region of the actinides. Pwu and Castel[64] developed the dynamical side of the calculation of the fission mass distribution as a function of the excitation energy of the compound nucleus on the basis of systematic two-dimensional calculations of the potential energy surfaces of the type of the two-center shell model. Introducing a certain shape of the initial wave packet, they expressed the total time-dependent wave function of the system in terms of an expansion with respect to stationary states. The expression for the mass distribution of the fission fragments was then found by substituting the fission lifetime into the final time-dependent wave function, which for spontaneous fission reduces to an expression similar to the one obtained from the theory of the WKB approximation for the barrier transmission. The results of this approach are also in good agreement with the experiments at high energies of the compound nucleus. Fong[65] also used calculations of the potential energy surfaces on the basis of the two-center shell model of Mustafa *et al.*[18] in his statistical theory of fission[66] and made a comparative study of the dynamical approach under a number of conditions, which also encompassed the approach proposed by Hasse.[67] He showed that whereas the statistical theory gives the principal features of asymmetric fission of ^{236}U, the dynamical theory is still far from this.

This distribution of the charge of the nucleus between the fission fragments has been calculated in the two-center shell model only in the framework of fragmentation theory[39] and will be described in detail below. Various authors[68] have put forward a number of empirical hypotheses such as equality of the charge distribution, nonvariation of the charge density, and maximum of the potential energy. Holub *et al.*[69] calculated the potential energy surfaces for charge vibrations in the ^{236}U nucleus using the two-spheroid liquid drop model of Nix and Swiatecki[70] and with allowance for shell effects calculated in a one-center potential by Strutinskiĭ's method. Facchini and Sassi[71] developed a statistical model of the mechanism of fragment separation and obtained charge distributions in general agreement with experiment.

We shall consider below our theory of the mass and charge distributions of the fission products, using the Hamiltonian of fragmentation theory. The calculations of the distributions are in excellent agreement with experiment.[35,39]

Theory of the mass and charge distributions of the

fission products. As we have already established above, we need to consider the fission dynamics only up to the point of fragment separation ($R<R_c$). In this case, assuming known the collective potential and the mass parameters, the problem reduces to direct quantization of Eq. (32). Solution of the corresponding Schrödinger equation gives the wave function, which then determines the evolution of the fission process. In practice, it is too complicated to do this for the case of all three collective coordinates, and therefore, as a first solvable problem, we reduce the problem to one with one collective coordinate.[33,35,39]

We assume the adiabatic approximation holds, i.e., the motions with respect to coordinates ξ and ξ_z are fast compared with the motion with respect to coordinate R (Ref. 72). This assumption is justified to the extent that the fragment nuclei emerge along the fission trajectory immediately after the process of penetration through the barrier has been completed. After this, they move rapidly under the influence of Coulomb repulsion, and the calculations of Refs. 18 and 38 show that the collective potential during this stage of the motion with respect to the coordinate R is almost independent of the asymmetry coordinates, so that the principal behavior of the mass and charge distributions of the fragments must be determined by the values of R at which the tunneling process of the fragments ceases. This fixes our choice of the values of R (or λ). Once the neck separating the fragments becomes narrow, the motion with respect to ξ and ξ_z is slowed down, and, finally, is frozen after the point of separation of the fragments. Thus, assuming complete adiabaticity, we can regard R (or λ) as a time-independent parameter. The coupling between the ξ and ξ_z motions is weak, so that in the first approximation they can be handled as independent of each other. The mass distributions are determined in this case as functions of ξ for fixed values of λ and ξ_z, and the charge dispersion is determined as a function of ξ_z for fixed values of λ and ξ.

To obtain the mass distribution, we write down the stationary Schrödinger equation found by quantizing[73] Eq. (32), in which the coordinates λ and ξ_z occur only as parameters:

$$\left(-\frac{\hbar^2}{2\sqrt{B_{\xi\xi}}}\frac{\partial}{\partial\xi}\frac{1}{\sqrt{B_{\xi\xi}}}\frac{\partial}{\partial\xi}+V(\lambda,\xi,\xi_z)\right)\Psi^{(\nu)}_{\lambda,\xi_z}(\xi)=E^{(\nu)}_{\lambda,\xi_z}\Psi^{(\nu)}_{\lambda,\xi_z}(\xi). \quad (37)$$

For the charge dispersion, we obtain an analogous equation after the substitution $\xi \rightleftarrows \xi_z$. Obviously, in this we neglect in (32) the terms with the coupling masses $B_{\lambda\xi}$ (and $B_{\lambda\xi_z}$). The vibrational states Ψ^{ν}_{λ} in the potential V are indicated by the quantum number $\nu = 0, 1, 2, \ldots$.

In the case of complete adiabaticity and in the case when the spontaneous fission takes place from the ground state of the nucleus, the system can only be in the lowest vibrational state $\nu = 0$. However, if fission takes place from excited states or subject to interaction between the λ, ξ, and ξ_z degrees of freedom, higher states with respect to ξ (or, accordingly, with respect to ξ_z) may be excited. Let us consider possible consequences of such excitations, assuming as a first step[35,39] a Boltzmann distribution for the population of the excited states:

$$|\Psi_\lambda|^2=\sum_{\nu=0}^{\infty}|\Psi^{(\nu)}_\lambda|^2\exp(-E^{(\nu)}_\lambda/\Theta), \quad (38)$$

where Θ, the nuclear temperature, is approximately related to the excitation energy through the semiempirical statistical relation[74]

$$E^*=(A/9)\Theta^2-\Theta,\ \text{MeV}. \quad (39)$$

In a more complete study of nuclear-temperature effects, we also use the cranking formula for the mass parameters generalized to finite temperature.[2]

The probability of finding a definite mass (or charge) fragmentation ξ (or ξ_z) at the position λ on the fission trajectory is proportional to $|\Psi_\lambda|^2$. To calculate the mass distributions,[35] this probability is compared with the mass yield Y with respect to the mass A_1 of one fragment ($d\xi = 2/A$) (Ref. 75):

$$Y(A_1)=|\Psi_\lambda(\xi(A_1))|^2\sqrt{B_{\xi\xi}(A_1)}\,[200/(A/2)]\ \text{(in percentages)} \quad (40)$$

and for the charge dispersion[39] this probability is compared with the yield of the separated charge Y with respect to the charge Z_1 of one fragment ($d\xi_z = 2/Z$):

$$Y(Z_1)=|\Psi_{\lambda\xi}(\xi_z(Z_1))|^2\sqrt{B_{\xi_z\xi_z}(Z_1)}\,(2/Z). \quad (41)$$

Below, both these yields are directly compared with experiment.

We consider further the generalization of these calculations[40] to the case when the time dependence of λ is taken into account. For example, for the mass asymmetry coordinate we write down the total wave function as a sum over Ψ^{ν}_{λ} with λ-dependent coefficients:

$$\Psi_\lambda(\xi)=\sum_\nu a_\nu(\lambda)\,\Psi^{(\nu)}_\lambda(\xi)\exp\left[-\frac{i}{\hbar}\int_0^t E^{(\nu)}_{\lambda(t)}\,dt\right]. \quad (42)$$

The expression (42) with $\lambda = \lambda(t)$ is merely an ordinary solution of the time-dependent Schrödinger equation:

$$\left[-\frac{\hbar^2}{2\sqrt{B_{\xi\xi}}}\frac{\partial}{\partial\xi}\frac{1}{\sqrt{B_{\xi\xi}}}\frac{\partial}{\partial\xi}+V\right]\Psi_{\lambda(t)}(\xi)=i\hbar\frac{\partial}{\partial t}\Psi_{\lambda(t)}(\xi). \quad (43)$$

For the motion with respect to the coordinate λ, one can obtain a classical equation. We calculate the average value of the energy (32) with respect to the wave function (42) with the kinetic and potential energies of the motion with respect to the coordinate ξ replaced by the expected value ξ of the Hamiltonian from (37). If the mass parameter $B_{\lambda\xi}$ of the coupling is ignored, this gives

$$\langle H\rangle_{\text{av}}=\tfrac{1}{2}\langle B_{\lambda\lambda}\rangle\dot{\lambda}^2+\sum_\nu|a_\nu(\lambda)|^2E^{(\nu)}_\lambda, \quad (44)$$

where the mass parameter averaged with respect to ξ has the form

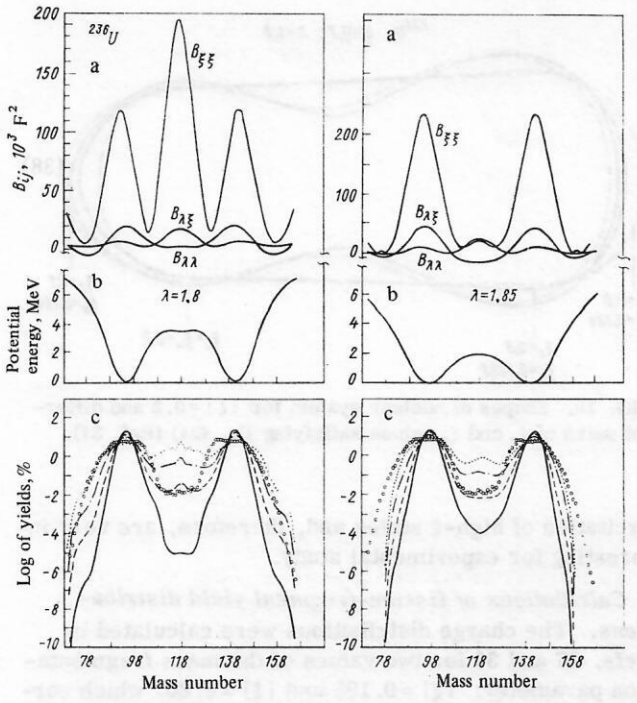

FIG. 7. Potential energy, mass parameters (in units of the nucleon mass), and theoretical fission product yields for ^{236}U for $\lambda = 1.8$ and 1.85. The experimental data are taken from Ref. 76. The continuous, dashed, dot-dash-dot, and dotted curves correspond, respectively, to the following values of the excitation energy: $E^* = 0$, 0.05, 1.0, and 7.0 MeV for $\lambda = 1.8$ and 0.0; 0.25, 0.5, and 1.25 for $\lambda = 1.85$ (Ref. 35).

$$\langle B_{\lambda\lambda}\rangle = \sum_{\nu,\mu} a_\nu^*(\lambda)\, a_\mu(\lambda) \int \Psi_\lambda^{(\nu)*}(\xi)\, B_{\lambda\lambda}(\lambda, \xi)\, \Psi_\lambda^{(\mu)}(\xi)\, \sqrt{B_{\xi\xi}}\, d\xi. \qquad (45)$$

The second term in the expression (44) is the effective potential of the relative motion. It depends on the probabilities of excitation of high-ξ states and, therefore, on the velocities $\dot\lambda$. Thus, this potential contains the effects of excitations during the motion with respect to the coordinate λ, which can be regarded as collective friction due to fragmentation, in contrast to ordinary friction due to excitation of single-particle states.

The dependence of the coefficients $a_\nu(\lambda)$ on the time is found, as usual, by substituting the wave function (42) into the time-dependent Schrödinger equation (43):

$$i\hbar \dot a_\nu = \sum_\mu \hbar\dot\lambda \left\langle \nu \left| \frac{\partial}{\partial\lambda} \right| \mu \right\rangle \exp\left[\frac{i}{\hbar}\int (E^{(\nu)} - E^{(\mu)})\, dt\right]. \qquad (46)$$

Equations (44) and (46) completely determine the problem. In practical calculations, however, the requirement of constancy of the total energy H is replaced by a relation with a parametrized force of friction:

$$dH/dt = -f\dot\lambda^2. \qquad (47)$$

This formalism can be applied in the same way to study the coupling of $\lambda(t)$ to the ξ_z motion. Below, we shall discuss the results of applying this method to the calculation of the mass yield distributions of the fission products, in particular, for the ^{236}U nucleus.

Calculations of fission-fragment mass yield distributions. These were calculated in Ref. 35 for fission of the nuclei ^{226}Ra, ^{236}U, and ^{258}Fm, which give typical examples of three-, two-, and one-hump distributions. Figure 7 shows the calculated potential energies, the mass parameters, and the mass yields for the ^{236}U nucleus for two values of λ and different temperatures; these were compared with the experimental data[76] for ^{235}U fission initiated by thermal neutrons. The potential energies are obtained as fairly smooth functions of the mass number and have the expected asymmetric minimum, whereas the mass parameters oscillate rapidly. The crossed mass parameter $B_{\lambda\xi}$ is fairly small, so that the assumption $B_{\lambda\xi}^2 \ll B_{\lambda\lambda}B_{\xi\xi}$ is well satisfied. It can be seen from Fig. 7 that the calculated distributions are in semiquantitative agreement with experiment. For fission from the ground state ($\Theta = 0$), the humps of the distribution are somewhat narrower, and the valley is too deep compared with the experimental data. This part of the calculations was first given in Ref. 33. Agreement was improved by introduction of excitations[35] into the system. Particularly pronounced is the raising of the valley with increasing temperature, and this, and also the simultaneous general flattening of the distribution when higher excitations are taken into account, agrees with the experimental data. The shape of the fragments corresponding to the minimum of the energy at the value $\lambda = 1.8$ is very similar to the shape shown in Fig. 6 for the case $\xi = \xi_z = \xi_n$ (for greater detail, see Ref. 33). Another important result is that the mass distributions are sensitive to only the total value of the mass parameters and depend weakly on the detailed form of their oscillations. A similar result is obtained in Ref. 35 for the nuclei ^{226}Ra and ^{258}Fm, which give three- and one-hump distributions, respectively (see Figs. 3 and 4 in Ref. 35). It should be emphasized that these results were found without any fitting of the parameters on the basis of the position and height of the peaks in the experimental distribution.

In Fig. 7 one can also note that for different values of λ the potential energy hardly changes, whereas the mass parameters have significant variations. Because of this, in Ref. 40, a study was made of the time dependence of λ [Eqs. (44)–(47)] for the case of ^{236}U fission. The calculations were made for several values of λ from 1.65 to 1.85 and for several values of the coefficient of friction f, which were chosen in such a way as to encompass the extreme cases of motion with respect to λ from unhindered acceleration to very slow motion (Fig. 8). It is found that an appreciable fraction of the collective behavior depends critically on the velocity λ and, therefore, on the friction. It can be seen from Fig. 8 that in the absence of friction the calculated yields of the fission products only slightly differ from one another for different values of λ and one may assume that the fragmentation takes place as before in the region of the barrier (impulse approximation). On the other hand, in the case of very strong friction and slow motion with respect to λ, the fission products yields follow the variations of the potential energy and the mass parameters during each stage of

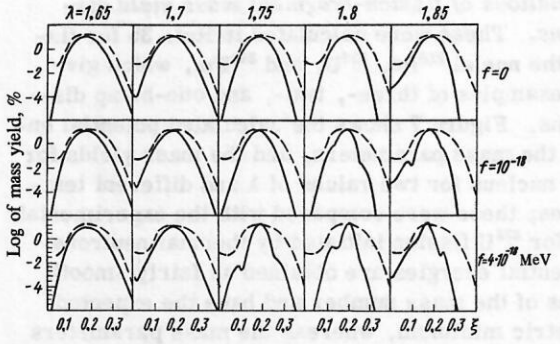

FIG. 8. Distribution of collective probability density $\Psi^*(\xi, \lambda)\Psi(\xi, \lambda)$ reduced to the equivalent mass yield for three different values of the coefficient of friction f (from top to bottom) and five values of λ (from left to right). Each column illustrates the changes of the wave function with different values of the friction for given λ; the dashed curves correspond to the calculations of Fig. 7 without allowance for the time dependence of λ (Ref. 71).

the variation of λ (adiabatic variation) and, because of the increase in the average value of $B_{\xi\xi}$, tend to become very narrow. The intermediate cases with regard to the strength of the friction exhibit a certain oscillatory fine structure (shoulders and bumps) of the final distributions, which arise because of the coherent

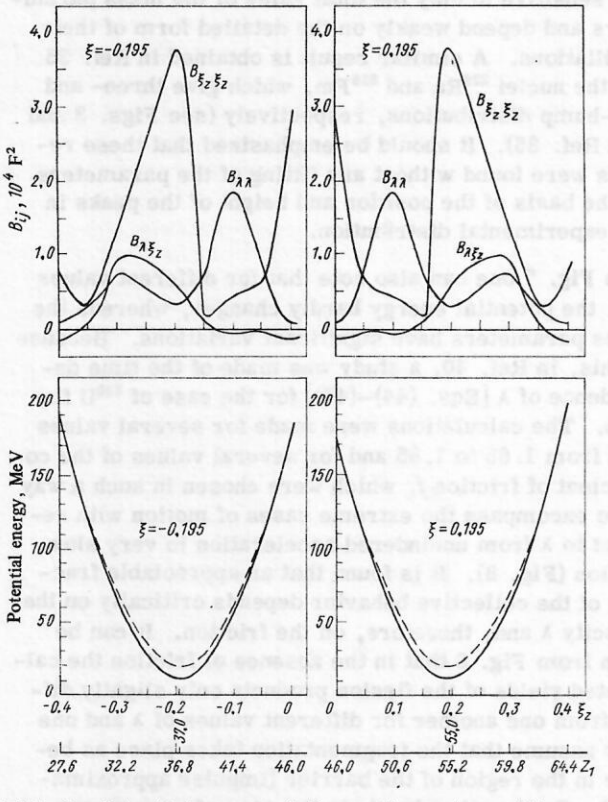

FIG. 9. Potential energy of charge dispersion and the mass parameters (in units of the nucleon mass) for $\xi = \pm 0.195$ in ^{236}U fission with $\lambda = 1.8$ (Ref. 39). The dashed curve is calculated on the basis of the liquid drop model; the continuous curve is calculated with allowance for shell effects.

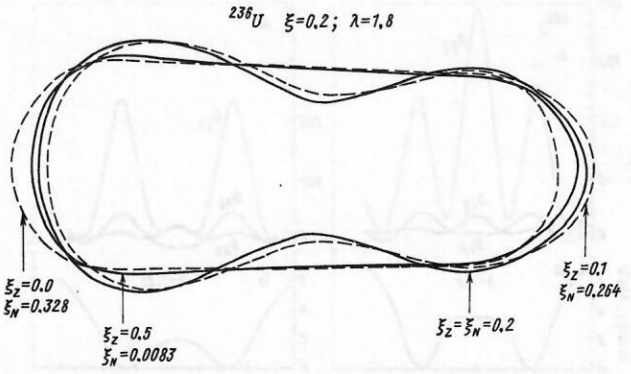

FIG. 10. Shapes of nuclear system for $|\xi| = 0.2$ and different pairs of ξ_z and ξ_n values satisfying Eq. (24) (Ref. 37).

excitation of high-ξ states and, therefore, are very interesting for experimental study.

Calculations of fission-fragment yield distributions. The charge distributions were calculated in Refs. 37 and 39 for two values of the mass fragmentation parameter: $|\xi| = 0.195$ and $|\xi| = 0.20$, which corresponds approximately to the mass chains $A_1 = 141$, $A_2 = 142$ and $A_1 = 142$, $A_2 = 94$ in ^{236}U fission. Figure 9 shows the results of calculations of the potential energy V and the mass parameters R_{ij} for the parameter values $\xi = \pm 0.195$ and $\lambda = 1.8$ of ^{236}U fission. The calculations for $|\xi| = 0.2$ lead to similar results.[37] An interesting aspect of these examples is that the potential energies have a single deep minimum at $\xi_z = \pm 0.195$ and $\xi_z = \pm 0.2$, respectively. Now in accordance with (24) we have $\xi = \xi_z = \xi_n$ in the region of the minimum, so that these examples confirm the conjecture that the charge distributions do not change arbitrarily, but follow the mass distribution. We recall that in the approach under consideration the protons and neutrons move in two separate potentials of the asymmetric two-center shell model, and one obtains a shape of the system with respect to ξ_z and, accordingly, with respect to ξ_n that does not differ too strongly from the shape of a system with given asymmetry ξ. Figure 6 shows the form of the proton and neutron systems with $\xi_z = 0.1$ and $\xi_n = 0.256$. These results refer to the mass asymmetry $\xi = 0.195$, for which the shape of the nuclear system, not shown in Fig. 6, lies between the proton and the neutron surfaces. For given ξ, the shape of the nuclear system will, of course, be different for different pairs of ξ_z and ξ_n values satisfying Eq. (24), as can be seen from Fig. 10 for the case $|\xi| = 0.2$. The results of the calculations for the mass parameters in Fig. 9 have the already known oscillating behavior, and only a very small region of their values around the minimum of the potential energy is important in the calculation of fission-fragment yield charge distributions. In addition, the mass coupling parameter $B_{\lambda\xi_z}$ is again small, and the inequality $B^2_{\lambda\xi_z} \ll B_{\lambda\lambda}B_{\xi_z\xi_z}$ is well satisfied, so that in (32) we can certainly ignore the coupling term, which is proportional to $B_{\lambda\xi_z}$, just as we did the term proportional to $B_{\lambda\xi}$ in the calculations of the mass distributions.

Figure 11 shows the experimental and calculated

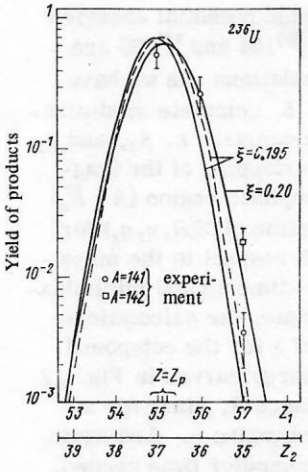

FIG. 11. Theoretical curves of charge dispersion for mass asymmetry $|\xi| = 0.195$ (mass chains 141 and 95) and $|\xi| = 0.20$ (chains 142 and 94) in ^{236}U fission. The dispersion curves are significantly changed for excitations of the system with $E^* \leqslant 7$ MeV. The experimental points are given only for the mass chains 141 and 142 (from Ref. 39). The dashed curve is calculated on the basis of the liquid drop model; the continuous curve is calculated with allowance for shell effects.

charge dispersions of the fission fragment yields for the cases $|\xi| = 0.195$ and $|\xi| = 0.20$. The calculations were made for several values of the temperature ($E^* \leqslant 7$ MeV), whose influence on the charge dispersion is not significant. The experimental data[77] are given only for the heavy mass chains $A_1 = 141$ and 142. The calculated curves of the charge dispersion over the fission fragments have a Gaussian form irrespective of the temperature of the nucleus. Both these results are in agreement with the experiments: It is known empirically that the experimental data for a given mass chain can be well represented by the Gaussian function

$$P(Z) = (c\pi)^{-1/2} \exp[-(Z - Z_p)^2/c], \qquad (48)$$

which is characterized by the most probable charge Z_p and the width c of the distribution and is insensitive to excitation energies of the compound nucleus less than 40 MeV (see, for example, Ref. 68). The empirical values of these parameters[77] for the mass chains 141 and 142 are $Z_p = 54$, 37, and $Z_p = 55$, 36, respectively, and the width, which is the same for both chains, is equal to $c = 0.9 \pm 0.1$. The theoretical curves have maxima at $Z = 55$ and $Z = 55.2$, respectively, and a width of the order their empirical values.

The influence of shell effects on the charge dispersion over the fission fragments was tested by calculations of the dispersion curve with allowance for the potential energy in the liquid drop model with a value $\xi = \pm 0.195$ (the dashed curve in Fig. 9). The results of such a calculation are shown by the dashed curve in Fig. 11, which gives somewhat better agreement with experiment. It must, however, be pointed out here that the experimental data in Fig. 11 refer to ^{235}U fission by thermal neutrons, whereas our calculations were made for spontaneous fission without allowance for evaporation of neutrons.[78] Calculations that include the effects of neutron evaporation and cases when the hypothesis of an unchanging charge distribution is not well satisfied are currently in the development stage. Recently, accurate measurements were made[79,80] of the charge distributions in light mass chains with a view to establishing the importance of pairing and odd-even effects. Application of fragmentation theory to these new data is a thing of the future.

To conclude this section, we recall once more that in our calculations parameters were not fitted to improve agreement with the experimental distributions. The calculations show that both the mass and chrage distributions of the fission fragments are determined primarily by the potential energy surfaces, whereas the mass parameters are responsible for details of the distributions such as the relationship between the humps and valleys, their heights and their widths, and also other fine structural details.

7. HEAVY-ION COLLISIONS

Heavy-ion collisions lead to more complicated and, therefore, more interesting mechanisms of nuclear interaction. One can have the most varied processes, such as, for example, the formation of nuclear molecules in elastic and inelastic scattering (briefly considered in Sec. 3); the formation of nuclear systems with large angular momenta; the formation in central collisions of heavy composite nuclei, which may provide a source for obtaining superheavy elements; fusion-fission reactions in which a heavy target nucleus and the incident particle fuse to form massive excited nuclei, which rapidly undergo fission and may have superheavy elements among their fission products; direct reactions involving transfer of one nucleon or a group of nucleons; deep inelastic reactions or quasi-fission reactions in which transfer products and fission fragments are observed; atomic and molecular phenomena associated with heavy ions. It is clear that some of these processes have particular mechanisms that are not related to one another. Others, however, exhibit a clear and smooth transition similar, for example, to the transition from the mechanism of one- and two-nucleon transfer through many-nucleon and cluster transfer to reactions of incomplete and, finally, complete fusion of nuclei. Reactions induced by heavy ions are intimately related to fission phenomena (as the inverse process). In both cases, the nuclear system is transformed (breaks up) into certain other nuclear systems. A difference is that in the case of fission the compound nucleus already exists, but in nucleus-nucleus collisions it must first be formed as an intermediate system, and then, depending on the energy, the angular momentum, the species of colliding nuclei, etc., one of the reaction mechanisms listed above is realized. In view of this commonality of the two phenomena, we shall consider the application of fragmentation theory to three types of reaction mechanism (formation of compound nuclei, fusion-fission, and quasi-fission) to which heavy-ion collisions lead. Direct transfer reaction have not hitherto been studied either experimentally or theoretically.

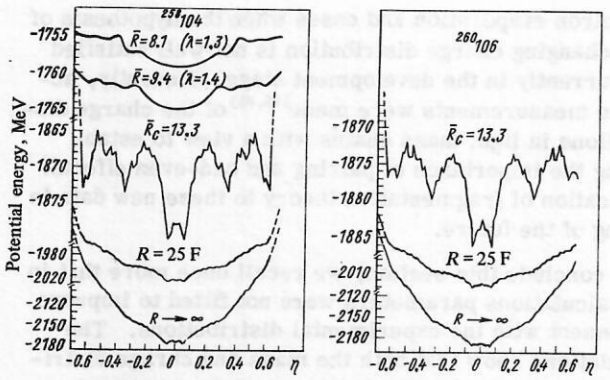

FIG. 12. Potential energies as functions of the mass asymmetry η and the relative distance R between the fragments for the compound systems $^{258}104$ and $^{260}106$. The curves for $R \geqslant R_c$ are calculated with minimization with respect to the charge asymmetry η_z except for the parts that are shown by the dashed curve. The energy scale is different for $R \leqslant R_c$ and $R > R_c$ (Ref. 41).

Formation of compound nuclei and the problem of obtaining superheavy elements. An important problem in the obtaining of superheavy elements via the preliminary formation of compound nuclei is the choice of an appropriate combination of target nucleus and incident particle. In their investigations, the group of scientists at Berkeley[81–85] bombard heavy deformed target nuclei with light spherical nuclei, while the group at Dubna[86–89] use spherical or nearly spherical but relatively heavy incident particles, directing them against deformed and spherical heavy targets. These two groups synthesized different isotopes of heavy elements with $Z = 102–106$. As was shown in Ref. 87, the cross sections for their production are so sensitive to the choice of the reaction partners that one cannot avoid confrontation with an important question: What is the optimal choice of the reaction partners in order to obtain a particular element? In what follows, we shall investigate this question on the basis of fragmentation theory.[41,43]

The idea of the method consists of making the choice of the reaction partners in such a way as to form a compound nucleus with minimal excitation energy. For cold compound nuclei, the number of emitted neutrons is not large, and, therefore, the cross section for the production of nuclei in the ground state must be large.[90] We shall illustrate our method by taking the example of the systems $^{258}104$ and $^{260}106$, which break up, say, after the evaporation of two neutrons, into the isotopes $^{256}104$ and $^{258}106$, respectively. Calculations were made for the compound nuclei formed in the collision of incident ions with $Z \geqslant 20$, and these therefore cannot be related to experiments with lighter particles.

Since one and the same compound system may be formed for different combinations of incident particles and target nuclei, we shall calculate the excitation energy of the compound system for all possible combinations. To do this in the framework of fragmentation theory, it is necessary to calculate the potential energy $V(R, \eta)$ as a function of the different values of the asymmetry parameters. The calculated potential energies $V(R, \eta)$ for the compound nuclei $^{258}104$ and $^{260}106$ are shown in Fig. 12. In these calculations, as we have already discussed above in Sec. 5, complete minimization with respect to the three parameters ε, β_1, and β_2 was realized in the region of overlapping of the fragments ($R < \bar{R}_c$), while in the asymptotic region ($R \geqslant \bar{R}_c$) Eq. (33) was used with minimization of $V(R, \eta, \eta_z)$ for each possible fragmentation with respect to the mass and the charge. Since the three-dimensional minimization procedure requires a long time, the calculations were made for only two values of λ for the compound nucleus $^{258}104$. The potential energy curves in Fig. 12 carry the mean value of the distance R, since for a fixed value of λ it changes with changing η. And again, because of the large amount of computer time needed, the calculations for $R > R_c$ (two curves) were made without minimization with respect to the coordinates η_z. The distance R_c of closest approach of the fragments was estimated by means of the empirical relation[91]

$$R_c = R_t + R_p + d, \tag{49}$$

where R_t and R_p are the radii of the target nucleus and the incident particle; d takes into account nuclear dynamical effects and for the heaviest combinations is of order ~1.7 F.

It can be seen in Fig. 12 that for both compound systems only a few values of η give a deep minimum in the potential energy. If the nuclei approach very close ($R \leqslant 7–8$ F) the minima are smoothed out and the potential energy becomes a more or less flat function of the mass asymmetry η. This is because the neck separating the fragments begins to disappear if they overlap strongly in the region $R \approx 8$ F, and the exact position of the separation plane, which determines the value of η, does not have great significance. An interesting feature of these calculations is that the deep minima in $V(R, \eta)$ for $R = R_c$ are not only stable with respect to η; in addition, new minima do not appear in the case of further overlapping of the nuclei with the formation of a compound system. Therefore, the potential energy $V(R = R_c, \eta, \eta_z)$, which can be readily calculated by means of (33), already gives the positions of the minima with respect to η and η_z. Slight shifts in the position of the determined minimum $V(\eta)$ or a change in its depth for a definite R may be attributed to the effects of charge dispersion over the fragments. Obviously, the appearance of the minima in the potential energy in Fig. 12 is due to the shell structure of the nuclei; at the same time, at least one of the two colliding nuclei is spherical. This fact is demonstrated in Fig. 13, in which we show the static deformations β_1 and β_2 as functions of η for the value $R = R_c$ (Ref. 62).

Further, to estimate the contribution of dynamical effects to the energy of the compound system we shall solve the stationary Schrödinger equation

$$H(\mathrm{R}, \eta, \eta_z, \alpha^{(1)}, \alpha^{(2)})\,\Psi = E\Psi \tag{50}$$

with initial asymptotic state ($R \to \infty$)

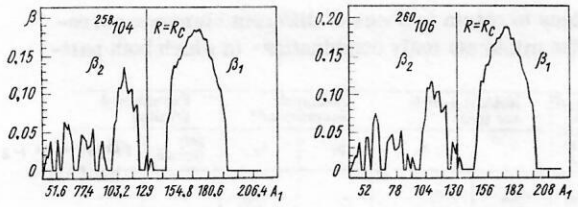

FIG. 13. Deformation parameters[62] for $R=R_c$ as functions of the mass numbers of two fragments.[41]

$$\Psi_i \sim \exp(ikz)\,\delta^{1/2}(\eta-\eta_0)\,\delta^{1/2}(\eta_z-\eta_{z0}) \times [\chi_{n1}(\alpha^{(1)}, \eta_0, \eta_{z0}) \otimes \chi_{n2}(\alpha^{(2)}, \eta_0, \eta_{z0})]. \quad (51)$$

The wave functions of δ type describe the states of mass and charge fragmentation; the functions χ_{n_1} and χ_{n_2} reflect the internal states of the nuclei of the ingoing channel determined by the values of η_0 and η_{z_0}; the surface vibrational states of the fragments are described by the wave functions $\alpha^{(1)}$ and $\alpha^{(2)}$. Since the static deformations β_1 and β_2 of the fragments depend strongly on the fragmentation coordinates η and η_z (see Fig. 13), in the Hamiltonian of the system there is a strong coupling between the surface vibrations and the mass and charge fragmentation. This means that in the case of changes of η and η_z when nucleons are transferred through the formation of a compound system the shapes of the nuclei of the ingoing channel may change, and this will be accompanied by a strong transfer of energy to the excitation of surface degrees of freedom.

Thus, it is necessary to distinguish two variants of the initial fragmentation that lead to different excitations of the compound system: 1) the original fragments (partner nuclei) are outside the minimum of the potential energy (see Fig. 12), which in accordance with Fig. 13 corresponds to the case $\beta_1 \neq 0$ and $\beta_2 \neq 0$, and 2) the initial fragments correspond to a minimum of the potential energy, and in such a case one or both of the nuclei are spherical.

In the first variant, with increasing overlapping of the nuclei of the ingoing channel there will be a transfer of a group of nucleons of large mass and charge with η and η_z changing in the direction of the minimum of the potential $V(\eta, \eta_z)$. According to classical mechanics, the transfer takes place under the influence of the "forces" $-\partial V/\partial\eta_z$. Since the nuclei change their shape as the system progresses toward the minimum, a large amount of energy will go into excitation of surface vibrational states. On the other hand, in the second variant mass and charge are not transferred when the nuclei approach one another since the "forces" $-\partial V/\partial\eta$ and $-\partial V/\partial\eta_z$ are now equal to zero. In this case, the dependence of the wave functions on η is approximately determined by the zero-point vibrations around the minimum of the potential energy. Thus, when the original fragments correspond to a minimum of $V(R, \eta, \eta_z)$, the excitation of surface degrees of freedom, i.e., of collective states, is significantly suppressed compared with the case when the initial fragments are taken outside the potential energy minimum. In this subsection we are interested in cases when minimal excitation energy is carried into the compound system and there is a high probability of fusion of the initial fragments; the case when nucleons are transferred will be studied below in the example of quasifission reactions.

Therefore, we have found that if the target nucleus and the incident nucleus correspond to a minimum of the potential energy $V(R, \eta, \eta_z)$ and, in addition, the energy of the bombarding particle allows the formation of a compound nucleus in a central collision, the excitation of the compound system must be minimal.

This method was applied for a large number of nuclei with $86 \leq Z \leq 122$ by means of calculations of the potential energy $V(R=R_c, \eta, \eta_z)$. In Table I we give the combinations of the incident particles and target nuclei that correspond to a minimum of V with respect to η and η_z and must lead to the synthesis of various new elements. Since in the general case the transfer of two protons between the fragments causes, because of charge dispersion effects, the acquisition or loss of energy of order 7–8 MeV, the table also contains neighboring combinations with ±2 protons (neutrons).

It is interesting to note that the combinations $^{50}_{22}$Ti + $^{206}_{82}$Pb, $^{50}_{22}$Ti + $^{208}_{82}$Pb and $^{54}_{24}$Cr + $^{206}_{82}$Pb, $^{54}_{24}$Cr + $^{208}_{82}$Pb predicted by Table I were used in the experiments at Dubna[87–89] to synthesize elements with $Z=104$ and 106, respectively, and a number of the combinations agree exactly with the experiments at Berkeley[92] proposed independently of the present calculations. Further, on the basis of estimates of the fission half-life Bengtsson *et al.*[93] proposed the combination $^{112}_{50}$Sn + $^{136}_{54}$Xe to obtain the element $Z=104$, which also agrees with our calculations. The fact that two different approaches to the problem of obtaining the element $Z=104$ under laboratory conditions indicate the combination of Sn and Xe strengthens confidence in the validity of our approach. In Table I we also give the quadrupole deformation parameters. As we have already noted above, in all combinations at least one of the two nuclei has a spherical shape. This fact agrees with the successful experiments at Dubna and Berkeley in which at least one of the two colliding was spherical.

The calculations we have presented do, however, require certain improvements. First, the change in the shape of the nuclei as a function of R in the region of the minimum of the potential energy will lead to the excitation of a compound system and, thus, rule out some of the combinations in Table I. Second, it is important to take into account effects associated with the temperture of the system and its rotation. Mustafa and Kumar[94] have extended the two-center shell model by including in it effects associated with angular momentum. They showed that the minima of the potential energy, the fission barriers, and the moments of inertia are fairly sensitive to the angular momentum. Fragmentation theory must still be generalized to this case.

Fusion-fission reactions. If a very heavy incident particle is scattered by a very heavy target nucleus, the resulting massive compound nucleus will immediately undergo fission. It is possible that new elements

TABLE I. Combinations of nuclei of the incident particle and the target nucleus to obtain isotopes of different elements corresponding to a minimum of the potential energy in the direct neighborhood of the minimum (only combinations in which both partners are stable in nature are given).

Element Z	Mass of compound nucleus, A	Incident particle and target A_1	A_2	Quadrupole deformations[62] β_1	β_2	Experimental situation performed	planned
102	256	^{48}Ca	^{208}Pb [a]	0	0	Yes[b]	Yes[92]
	254	^{46}Ca	^{208}Pb	0	0	—	—
		^{48}Ca	^{206}Pb [a]	0	0	Yes[b]	—
		^{124}Sn	^{130}Te [a]	0	0	—	—
	252	^{46}Ca	^{206}Pb	0	0	—	—
		^{48}Ca	^{204}Pb [a]	0	0	Yes[b]	—
		^{82}Se	^{170}Er	0	0.190	—	—
		^{122}Sn	^{130}Te [a]	0	0	—	—
		^{124}Sn	^{128}Te [a]	0	0	—	—
	250	^{46}Ca	^{204}Pb	0	0	—	—
		^{50}Ti	^{200}Hg	0	−0.037	—	—
		^{86}Kr	^{164}Dy [a]	0	0.179	—	—
		^{120}Sn	^{130}Te	0	0	—	—
		^{122}Sn	^{128}Te [a]	0	0	—	—
		^{124}Sn	^{126}Te	0	−0.035	—	—
104	260	^{124}Sn	^{136}Xe [a]	0	0	—	Yes[92]
		^{130}Te	^{130}Te [a]	0	0	—	—
	258	^{50}Ti	^{208}Pb [a]	0	0	Yes[87]	—
		^{82}Se	^{176}Yb	0	0.186	—	—
		^{122}Sn	^{136}Xe [a]	0	0	—	—
		^{124}Sn	^{134}Xe [a]	0	0	—	—
		^{128}Te	^{130}Te [a]	0	0	—	—
104	256	^{50}Ti	^{206}Pb [a]	0	0	Yes[88]	—
		^{86}Kr	^{170}Er [a]	0	0.190	—	—
		^{120}Sn	^{136}Xe	0	0	—	—
		^{122}Sn	^{134}Xe [a]	0	0	—	—
		^{124}Sn	^{132}Xe	0	0	—	—
	254	^{50}Ti	^{204}Pb [a]	0	0	—	—
		^{86}Kr	^{168}Er [a]	0	0.186	—	—
		^{118}Sn	^{136}Xe	0	0	—	—
		^{120}Sn	^{134}Xe [a]	0	0	—	—
		^{122}Sn	^{132}Xe	0	0	—	—
106	266	^{130}Te	^{136}Xe [a]	0	0	—	Yes[92]
	264	^{128}Te	^{136}Xe	0	0	—	—
		^{130}Te	^{134}Xe	0	0	—	Yes[92]
	262	^{54}Cr	^{208}Pb [a]	0	0	Yes[89]	—
		^{86}Kr	^{176}Yb [a]	0	0.186	—	—
		^{124}Sn	^{138}Ba [a]	0	0	—	—
		^{126}Te	^{136}Xe	−0.035	0	—	—
		^{128}Te	^{134}Xe [a]	0	0	—	—
		^{130}Te	^{132}Xe	0	0	—	—
	260	^{54}Cr	^{206}Pb [a]	0	0	Yes[89]	—
		^{86}Kr	^{174}Yb [a]	0	0.188	—	—
		^{122}Sn	^{138}Ba [a]	0	0	—	—
		^{124}Sn	^{136}Xe	0	0	—	—
		^{126}Te	^{134}Xe	−0.035	0	—	—
	258	^{54}Cr	^{204}Pb [a]	0	0	—	—
		^{86}Kr	^{172}Yb [a]	0	0.189	—	—
		^{88}Sr	^{170}Er	0	0.190	—	—
		^{120}Sn	^{138}Ba [a]	0	0	—	—
		^{122}Sn	^{136}Ba	0	0	—	—
106	258	^{124}Te	^{134}Xe	−0.056	0	—	—
		^{126}Te	^{132}Xe [a]	−0.035	0	—	—
		^{128}Te	^{130}Xe	0	0	—	—
108	272	^{136}Xe	^{136}Xe [a]	0	0	—	—
	270	^{134}Xe	^{136}Xe [a]	0	0	—	—
	268	^{82}Se	^{186}W	0	0.146	—	—
		^{130}Te	^{138}Ba [a]	0	0	—	—
		^{132}Xe	^{136}Xe [a]	0	0	—	—
		^{134}Xe	^{134}Xe [a]	0	0	—	—
	266	^{58}Fe	^{208}Pb	0	0	—	—
		^{82}Se	^{184}W	0	0.155	—	—
		^{86}Kr	^{180}Hf [a]	0	0.171	—	—
		^{130}Te	^{136}Ba	0	0	—	—
		^{132}Xe	^{134}Xe [a]	0	0	—	—
110	280	^{48}Ca	^{232}Th	0	0.123	—	—
	274	^{136}Xe	^{138}Ba [a]	0	0	—	—
	272	^{64}Ni	^{208}Pb	0	0	—	—
		^{82}Se	^{190}Os	0	0.122	—	—
		^{86}Kr	^{186}W [a]	0	0.146	—	—
		^{134}Xe	^{138}Ba [a]	0	0	—	—
		^{136}Ba	^{136}Xe	0	0	—	—
	270	^{64}Ni	^{206}Pb [a]	0	0	—	—
		^{86}Kr	^{184}W [a]	0	0.155	—	—
		^{130}Te	^{140}Ce	0	0	—	—
		^{132}Xe	^{138}Ba [a]	0	0	—	—
		^{134}Xe	^{136}Ba	0	0	—	Yes[92]
	268	^{64}Ni	^{204}Pb [a]	0	0	—	—
		^{86}Kr	^{182}W [a]	0	0.165	—	—
		^{88}Sr	^{180}Hf	0	0.171	—	—
110	268	^{128}Te	^{140}Ce	0	0	—	—
		^{130}Xe	^{138}Ba [a]	0	0	—	—
		^{132}Xe	^{136}Ba [a]	0	0	—	Yes[92]
		^{134}Ba	^{134}Xe	0	0	—	—
112	286	^{48}Ca	^{238}U	0	0.136	—	—
	284	^{48}Ca	^{236}U	0	0.132	—	—
	282	^{48}Ca	^{234}U [a]	0	0.128	—	—
	280	^{48}Ca	^{232}U [a]	0	0.123	—	—
	278	^{70}Zn	^{208}Pb	0	0	—	—
		^{76}Ge	^{202}Hg	0.060	0	—	—
		^{82}Se	^{196}Pt	0	0.064	—	—
		^{86}Kr	^{192}Os	0	0.109	—	—
		^{136}Xe	^{142}Ce	0	0	—	—
114	292	^{48}Ca	^{244}Pu	0	0.150	—	Yes[92]
	290	^{48}Ca	^{242}Pu	0	0.145	—	—
	288	^{48}Ca	^{240}Pu [a]	0	0.140	—	—
	286	^{48}Ca	^{238}Pu [a]	0	0.136	—	—
		^{136}Xe	^{150}Nd [a]	0	0.124	—	—
	284	^{48}Ca	^{236}Pu [a]	0	0.132	—	—
		^{76}Ge	^{208}Pb	0.060	0	—	—
		^{82}Se	^{202}Hg	0	0	—	—
		^{86}Kr	^{198}Pt	0	−0.035	—	—
		^{124}Sn	^{160}Gd [a]	0	0.162	—	—
		^{134}Xe	^{150}Nd	0	0.124	—	—
		^{136}Xe	^{148}Nd [a]	0	0.099	—	—

[a] Combinations corresponding to a minimum in $V(R, \eta, \eta_Z)$. The cross sections for this case are comparatively large.
[b] Added after completion of the paper (taken from: G. N. Flerov *et al.*, Preprint JINR D7-9555 [in Russian], Dubna (1976)).

are included among the fission products. Reactions with this mechanism were studied in fragmentation theory for the compound systems $^{322}128$, $^{416}164$, and $^{476}184$ (Refs. 36, 38, and 44). It was of interest to chose precisely these systems because they include the following combinations, respectively, of incident particles and target nuclei: $^{84}Kr + ^{238}U$, $^{208}Pb + ^{208}Pb$, and $^{238}U + ^{238}U$. For the reaction $^{84}Kr + ^{238}U$, the mass distribution was measured[95] in the range $67 \leq A \leq 239$, but instead of discovering new superheavy elements the investigation of this reaction led to the discovery of a new phenomenon, the so-called quasifission. The other two reactions have not yet been explained in the framework of existing mechanisms.

As an example, in Fig. 14 we give the results of calculation of the potential energy $V(R, \eta)$ for the compound system $^{476}184$. The calculations for the other two systems can be found in Refs. 36 and 38. It can be seen from Fig. 14 that the number of deep minima in $V(\eta)$ related to the shell structure of the nuclei is almost independent of the distance R between the fragments. The fragments corresponding to minima of the potential energy in the three compound systems are given in Table II. It is interesting that superheavy elements appear as fission products in the system $^{476}184$ and in the experimentally unmeasured region of masses of the system $^{322}128$. The compound system $^{416}164$ has only one minimum of the potential energy at $\eta = 0$ in the investigated region $|\eta| = 0.2$. Because it is now becoming possible to accelerate ever heavier ions, it will be necessary to make further study of fusion-fission reactions.

Quasifission reactions. Recently, measurements were made of the mass distributions of the products for certain reactions induced by heavy ions[95,95] that have become known as quasifission reactions. These measurements gave additional information about reaction characteristics known earlier from the measurements

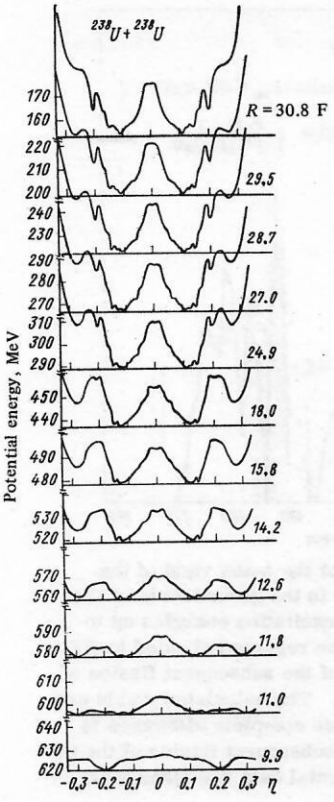

FIG. 14. Adiabatic potential energy $V(R, \eta)$ for the compound system $^{476}184$ (Ref. 44).

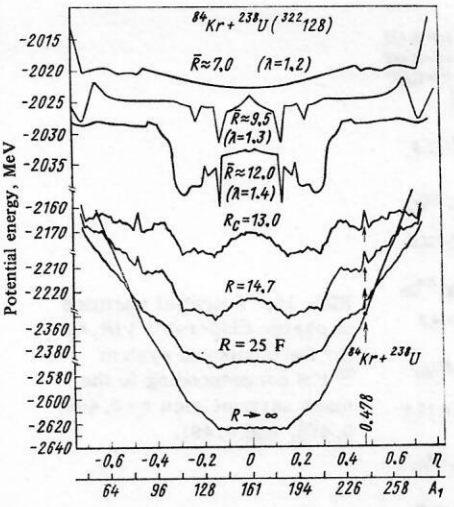

FIG. 15. Potential energy as function of the mass asymmetry and the relative distance R for the compound system $^{84}Kr+^{238}U\rightarrow^{322}128$. The curves for $R\geq R_c$ were calculated with minimization with respect to the charge asymmetry η_z. The energy scale is different for $R>R_c$ and $R\geq R_c$.

of Refs. 97–99: 1) Two product yields are observed with masses near the masses of the incident nucleus and target nucleus; 2) the kinetic energies of the fragments (in the center-of-mass system) have values close in magnitude to the energy of the Coulomb repulsion between two fragments of an ordinary fission process; and 3) the angular distributions of the reaction products are narrow and form a peak at an angle that is slightly less than the classical turning (contact) angle and thus differ from the angular distributions of reactions involving complete fusion and fission. Here, a first attempt is made to interpret the observed mass distribution in the $^{84}Kr+^{238}U$ reaction on the basis of fragmentation theory. Preliminary results of this investigation have already been given in Refs. 45 and 46.

The radiochemical method was used to measure the yields of 156 nuclei, which were identified only by Z and A, resulting from the scattering of 605-MeV ^{84}Kr ions on ^{238}U. The final mass yields were determined by integration, for each mass number, of the Gaussian charge-dispersion curves, which were fitted on the basis of the experimental data. This analysis reveals the following five components of the mass distribution:

TABLE II. Fragments corresponding to a minimum of the potential energy.

System A_Z	$\|\eta\|$	Fragments A_1	Fragments A_2	System A_Z	$\|\eta\|$	Fragments A_1	Fragments A_2
$^{322}128$	0.130	$^{182}_{72}$Hf	$^{140}_{56}$Ba	$^{416}164$	0	$^{208}_{82}$Pb	$^{208}_{82}$Pb
	0.155	$^{186}_{74}$W	$^{136}_{54}$Xe	$^{476}184$	0.110	$^{264}102$	$^{212}_{82}$Pb
	0.292	$^{208}_{82}$Pb	$^{114}_{46}$Pd		0.134	$^{270}104$	$^{206}_{80}$Hg
	0.466	$^{236}_{92}$U	$^{86}_{36}$Kr		0.197	$^{285}112$	$^{191}_{72}$Hf
	0.702	$^{274}108$	$^{48}_{20}$Ca		0.231	$^{293}114$	$^{183}_{70}$Yb

Near the masses of the target nucleus and the incident particle are concentrated products associated with transfer of nucleons (distribution of rabbit-ear type); at around $A\approx 85$ there is a product yield of quasi-Kr type; there is a concentration of product yield somewhat lower than the value $A=119$ corresponding to symmetric fission of the (missing) quasi-U component; around $A\approx 140$ there is observed a yield of a heavy mass branch of products of low-energy fission of nuclides with $Z\approx 92$; there are fragments from the complete fusion-fission reaction (broad extended distribution of products in the region $A\approx 160$–180); and a yield spike at $A=195$ (sometimes known as the "gold finger"). Below, to explain this reaction, we propose a two-step mechanism: fission after transfer of several nucleons. In this approach, there are no free parameters to be fitted by the experimental data.

The results of calculations of the potential energy $V(R,\eta)$ for the compound system $^{322}128$ with original fragmentation $^{84}Kr+^{238}U$ determined by the value $\eta=0.478$ are given in Fig. 15. The potential energies $V(R, \eta_z)$ of the charge dispersion for the original system $|\eta|=0.478$ and neighboring values ($|\Delta A|=2$) $|\eta|=0.466$ and 0.491 are given in Fig. 16. It should be noted that all calculations were made with the step $|\Delta A|=|\Delta Z|=2$ and, therefore, do not contain any interpolation procedure. It can be seen from Figs. 15 and 16 that the combination $^{84}Kr+^{238}U$ in the limit $R\rightarrow\infty$ and as the nuclei approach always lies outside the minimum of the potential energy of the corresponding compound system. In such a case, the "transfer forces" $-\partial V/\partial\eta$ and $-\partial V/\partial\eta_z$ are not equal to zero and nucleons are transferred between the fragments in the direction of variation of η and η_z to the values corresponding to the minimum of the potential energy (as described above). The fact that transfer takes place is clearly demonstrated in the application of our theory of the charge distribution of the fission product yield

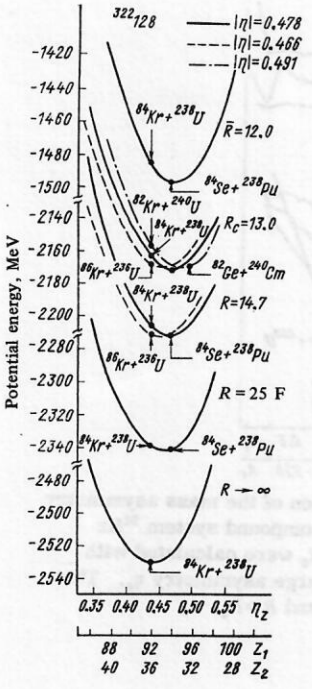

FIG. 16. Potential energies of charge dispersion $V(R, \eta_z)$ for the compound system $^{322}128$ corresponding to the mass asymmetries $\eta = 0.466$, 0.478, and 0.491.

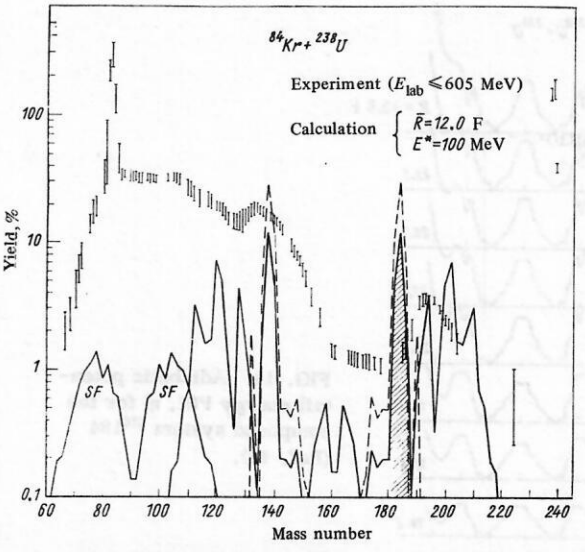

FIG. 18. Results of calculation of the mass yield of the $^{84}Kr + ^{238}U$ reaction for $\bar{R} = 12.0$ F in the ground state of the system (dashed curves) and with excitation energies up to 100 MeV (continuous curves). The regions indicated by SF were obtained from calculations of the subsequent fission of the hatched component at $A \approx 184$. The calculated yields are not normalized to experiment since complete allowance is not made for the yields from the subsequent fission of the primary components. The experimental data are taken from Ref. 95.

(see Sec. 7) to fission of the system $^{322}128$ with values $|\eta| = 0.478$ and $\bar{R} = 12$ (Fig. 17). The most probable values of the charge are here $Z_p = 34$ and 94. Since the highest probability for the transfer process occurs when $R \approx R_c$, analysis of the potential energy $V(\eta_z, R = R_c)$ in Fig. 16 also indicates that the systems in the potential energy minimum with values $|\eta| = 0.466$, 0.478, and 0.491 arise when there is transfer of respectively two neutrons, two protons, and four protons and the energy needed for the transfer of two neutrons is the lowest. Therefore, there will arise products of the transfer near ^{86}Kr and ^{236}U, which explain one of the main features of the quasifission reaction, namely: observation of products centered on the mass values of the incident nucleus and the target nucleus (rabbit ears).

During the transfer process, the shape of the nuclei changes and a certain amount of energy may be expended on the excitation of surface vibrational states. This will be elucidated by an analysis of the result of fission of the compound system formed after the transfer. The assumption that a compound system is formed is confirmed by the observation noted above of the characteristic kinetic energies of the reaction products. This fact suggests the following ideas: The initial kinetic energy is almost completely redistributed during the time of collision of the two original nuclei; there is formed a composite strongly deformed system (more deformed than the shape of the system in the saddle point in the case of ordinary fission); the strong Coulomb repulsion between the two parts of the composite system tends to tear it apart; a neck is formed in the system and, finally, fragments are separated in a shape similar to the one realized at the point of separation in the case of ordinary fission. Proceeding from this picture, we calculate as the second step the mass (and charge) distributions for fission of the system $^{322}128$ in the same way as we did for normally fissioning nuclei (see Sec. 7).

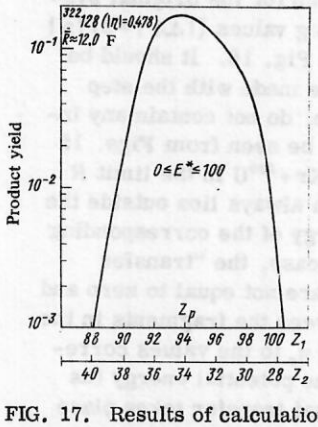

FIG. 17. Results of calculations of the charge distribution of the product yield with mass-asymmetry value $|\eta| = 0.478$ for fission of the system $^{322}128$ with the value $\bar{R} = 12.0$ F and excitation energies $0 \leqslant E^* \leqslant 100$ MeV.

The calculated mass yields Y (in percentages) for fission of the system $^{322}128$ for $\bar{R} = 12$ F from the ground state (dashed curve) and from states with excitation energies up to 100 MeV above the Coulomb barrier (continuous curves) are shown in Fig. 18. The effect of introducing excitations is obviously large, although the distribution is hardly changed by variation of the energy. We have calculated the yields only for $\bar{R} = 12$ F since this value corresponds to the configuration at the time of separation of the fragments. Figure 18 shows

the experimental data[95] for scattering of ^{84}Kr ions with energy 605 MeV (in the laboratory system) on a thick ^{238}U target, obtained by radiochemical analysis. Our calculations give the following components of the mass distribution: sharp peaks of the reaction product yields at $A \approx 114$, 120, 128, 132, 138, 184, 190, 194, 202, and 208 and a number of enhancements of the product yield between $A \approx 142$ and 180. Obviously, some of these yields correspond to the experimentally established components, namely, the following features are present: a concentration of the product yield somewhat lower than the value $A \approx 119$ from symmetric fission of the (missing) quasi-U component; a product yield at $A \approx 140$, which is a component of the heavy product of low energy fission of nuclides with $Z = 92$; and a "gold finger" at $A \approx 195$. The broad extended distribution of products observed experimentally in the region $A \approx 160$–180 is manifested in our calculations as a number of enhancements in the range $A \approx 142$–180. The four additional components in our calculations at $A \approx 184$, 190, 202, and 208 undergo, we must assume, secondary fission.

We consider in detail the subsequent fission of only the component at $A \approx 184$ (in Fig. 18 shown by the hatching), which leads to the appearance of a product yield of $A \approx 80$ and 104 (denoted in Fig. 18 as SF). Obviously, these mass yields correspond to the experimental yield of products of quasi-Kr fission and the light mass branch of low-energy fission of nuclides with $Z = 92$ (not fitted in the experiment). We also have calculations of the potential energy surfaces for the fission of the other two products at $A \approx 202$ and 208, on the basis of which one can assume that the fission of these products gives components at $A \approx 68$, 76, 82, 120, 126, and 134 for $A \approx 202$ and at $A \approx 74$, 82, 126, and 134 for $A \approx 208$. Some of these components will obviously augment the primary components analyzed above and thus improve the agreement between our calculations of the mass yields and the experimental data. It must, however, be noted that some of the components analyzed in the experimental data as a result of subsequent fission appear in our calculations as principal fission products. A more accurate quantitative comparison with the existing data is as yet not particularly meaningful since: 1) the experimentally measured independent and cumulative yields are as yet only part of the total mass yield; 2) the experimental data were analyzed under the assumption that the charge distributions have a Gaussian shape whereas our (preliminary) calculations give two-hump distributions as well for this reaction; 3) in our calculations it is necessary to take into account effects associated with R motion, evaporation of neutrons, charge dispersion, finite changes in the impact parameter, and so forth. Therefore, the two-step mechanism of "transfer of several nucleons and subsequent normal fission" investigated here is in qualitative agreement with the experimental picture of the quasifission reaction.

Charge distribution of products in heavy-ion collisions. Let us consider the application of our theory of charge dispersion (see Sec. 7) to reactions induced by heavy ions. Recently, measurements have been made[100,101] of the charge distributions of the product yields of several reactions induced by heavy ions that have become known as quasifission reactions. An interesting result of these measurements is that, besides the ordinary charge distributions of Gaussian type, two-hump distributions were also observed. In particular, in the reactions $^{84}_{36}\mathrm{Kr} + {}^{65}_{29}\mathrm{Cu} \rightarrow {}^{149}_{65}\mathrm{Tb}$ and $^{136}_{54}\mathrm{Xe} + {}^{209}_{83}\mathrm{Bi} \rightarrow {}^{245}137$ charge distributions of Gaussian shape were observed around $Z \approx 32$ and $Z \approx 54$ (Refs. 100 and 101). On the other hand, in the reaction $^{40}_{18}\mathrm{Ar} + {}^{109}_{47}\mathrm{Ag} - {}^{149}_{65}\mathrm{Tb}$ the observed charge distribution of products[100] was split into two groups: one concentrated at $Z \approx 32$ corresponding to symmetric fission of the compound nucleus, and the other centered around $Z \approx 18$. Our calculations of the fission of the compound nucleus $^{322}128$ for the mass chains corresponding to the values $|\eta| = 0.478$, 0.21, and 0.13 agree with these experimental results. However, our calculations are only preliminary.

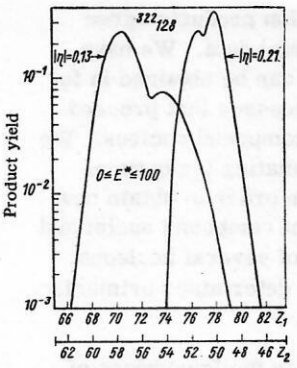

FIG. 19. Results of calculation of charge distributions of product yield in fission of the system $^{322}128$ with mass asymmetry $|\eta| = 0.21$ and 0.13 and excitation energies $0 \le E^* \le 100$ MeV.

The typical potential energy of the charge dispersion has already been given in Fig. 16 and agrees completely with the potential energy shown in Fig. 9 for normally fissioning nuclei. The calculated charge distribution of the product yield in the case of fission of the system $^{322}128$ with the value $|\eta| = 0.478$ (see Fig. 17) has a Gaussian shape with most probable charges $Z_p = 34$ and 94. At the same time, the charge yields calculated for the values $|\eta| = 0.21$ and $|\eta| = 0.31$ for the same system $^{322}128$ give the two-hump distributions shown in Fig. 19. The peaks are centered at $Z \approx 77$ and 78 (51 and 50 for the corresponding light mass chains) for the value $|\eta| = 0.21$ and at $Z \approx 71$ and 74 (or 57 and 54) for the value $|\eta| = 0.13$. From our calculations we may conclude that, first, the effects of charge dispersion in heavy-ion collisions are small and of the same order as in normal fission and, second, our calculations of the charge distributions for the quasifissioning compound system $^{322}128$ are in very good agreement with the observed characteristics in the quasifission reactions. Verification of these calculations and conclusions is a matter for the future.

CONCLUSIONS

Thus, we have been able to show that the two-center shell model and fragmentation theory considered here give a very successful and unified description of nuclear fission and heavy-ion collisions. The mass and

charge distributions of the reaction products agree quantitatively with the experimental data. We have shown that superheavy elements can be obtained in fusion-fission reactions and in processes that proceed through the formation of a cold compound nucleus. We have proposed a method for calculating the optimal choice of the reaction partners in order to obtain new elements through the formation of compound nuclei and also for the process of transfer of several nucleons. The major part of our results is determined primarily by the potential energy surfaces.

Other interesting applications in the framework of the two-center shell model are investigations of the formation of nuclear molecules and the successful description of the elastic scattering cross section[102] of the reaction $^{16}O + ^{12}C$.

In view of the success of the first applications of fragmentation theory it would be worthwhile considering some of its future prospects. Obviously, the potential energy must be calculated with allowance for the effects of the nuclear temperature and rotation. In such a case, the calculations of the mass parameters must also be generalized to the case of finite temperatures.[2] Further, it is important to modify fragmentation theory so as to reflect the detailed differences between fission processes and heavy-ion collisions. Thus, the surface-energy term used in the fission problem and taken from the expression for the energy in the liquid drop model must be modified to describe the scattering process.[103] The deformation parameters of the fragments must occur in the theory as dynamical coordinates, since the shape of the nuclei changes from the shape of the nuclei on the fission trajectory as they approach one another. It is also important to take into account the influence of nonadiabatic effects on the mass parameters. An alternative way of allowing for these effects, which are called polarization effects, is to use velocity-dependent potentials that would describe in a different manner the relative motion in the ingoing and outgoing channels. Finally, it is desirable to have a complete dynamical theory of fission and heavy-ion collisions containing a dependence on the time and on the excitation energy of the system. As we mentioned in the introduction, first attempts in this direction were already made in Ref. 47. And, last of all, it is no less important to take into account the effects of energy dissipation due to friction and viscosity of the nuclear medium.[104]

Direct generalizations of the two-center shell model to models with three or more centers are considered in Ref. 105. So far, a three-center shell model has been used only in the problem of ternary fission[106] and in investigations of the cluster structure of light nuclei.[107] In order to describe three-particle phenomena in the concepts of fragmentation theory, it is necessary to introduce into the theory two mass-asymmetry coordinates and two charge-asymmetry coordinates. In this case, the scattering theory becomes more complicated since it is necessary to consider two or more particles in the continuum.

I should like to thank Professor W. Greiner for his assistance in my study of these questions, for his collaboration, and for his support during this work. I also thank Professor W. Sheid and A. Săndelescu and other colleagues for numerous helpful suggestions and discussions. Finally, I thank Mrs. Hall and Mrs. Lassarig for their work reprinting the material and Mrs. B. Utschig for drawing the figures.

[1]S. G. Nilsson *et al.*, Nucl. Phys. A 131, 1 (1969).
[2]M. Brack *et al.*, Rev. Mod. Phys. 44, 320 (1972).
[3]M. Bolsterli *et al.*, Phys. Rev. C 5, 1050 (1972).
[4]V. V. Pashkevich, Nucl. Phys. A 169, 275 (1971).
[5]E. Merzbacher, Quantum Mechanics, Wiley, New York (1961), pp. 64–77.
[6]N. A. Cherdantsev and V. E. Marshalkin, Izv. Akad. Nauk. SSSR, Ser. Fiz. 30, (1966).
[7]M. Demeur and G. Reidemeister, Ann. de Phys. (Paris) 1, 181 (1967).
[8]P. Holzer, U. Mosel, and W. Greiner, Nucl. Phys. A 138, 241 (1969).
[9]D. Scharnweber, U. Mosel, and W. Greiner, Phys. Rev. Lett. 24, 601 (1970).
[10]K. Albrecht *et al.*, Phys. Lett. B 32, 229 (1970).
[11]D. Scharnweber, W. Greiner, and U. Mosel, Nucl. Phys. A 164, 257 (1971).
[12]U. Mosel, J. Maruhn, and W. Greiner, Phys. Lett. B 34, 587 (1971).
[13]J. Maruhn and W. Greiner, Z. Phys. 251, 431 (1972).
[14]W. Fabian, G. E. W. Horlacher, and K. Albrecht, Nucl. Phys. A 190, 533 (1972).
[15]U. Mosel and D. Scharnweber, Phys. Rev. Lett. 25, 678 (1970).
[16]U. Mosel and H. W. Schmitt, Nucl. Phys. A 165, 73 (1971); Phys. Rev. C 4, 2185 (1971).
[17]U. Mosel, Phys. Rev. C 6, 971 (1972).
[18]M. G. Mustafa, U. Mosel, and H. W. Schmitt, Phys. Rev. Lett. 28, 1536 (1972); Phys. Rev. C 7, 1519 (1973); M. G. Mustafa, Preprint, University of Maryland.
[19]C. Y. Wong, Phys. Lett. B 30, 61 (1969).
[20]B. L. Anderson, G. Dickmann, and K. Dietrich, Nucl. Phys. A 159, 337 (1970).
[21]G. D. Adeev, P. A. Cherdantsev, and I. A. Gamalya, Phys. Lett. B 35, 125 (1971).
[22]B. Slavov, J. E. Galonska, and A. Faessler, Phys. Lett. B 37, 483 (1971); B. Slavov and A. Faessler, Z. Phys. 271, 161 (1974).
[23]T. A. Johansson, Nucl. Phys. A 183, 33 (1972).
[24]D. E. Maharry and J. P. Davidson, Nucl. Phys. A 183, 371 (1972).
[25]K. Albrecht, Nucl. Phys. A. 207, 225 (1973).
[26]A. Iwamoto *et al.*, Progr. Theor. Phys. 55, 115 (1976).
[27]V. M. Strutinskii (Strutinsky), Nucl. Phys. A 95, 420 (1967); 122, 1 (1968).
[28]K. Pruess and W. Greiner, Phys. Lett. B 33, 197 (1970).
[29]U. Mosel, T. D. Thomas, and P. Riesenfeldt, Phys. Lett. B 33, 565 (1970).
[30]T. Morovic and W. Greiner, Z. Naturforsch. Teil A 31, 327 (1976).
[31]H. W. Schmitt and U. Mosel, Nucl. Phys. A 186, 1 (1972).
[32]M. G. Mustafa and H. W. Schmitt, Phys. Rev. C 8, 1924 (1973).
[33]P. Lichtner *et al.*, Phys. Lett. B 45, 175 (1973); in Phys. and Chem. Fission, IAEA SM-174/102 (1973).
[34]H. J. Fink *et al.*, Z. Phys. 268, 321 (1974).
[35]J. Maruhn and W. Greiner, Phys. Rev. Lett. 32, 548 (1974).
[36]H. J. Fink *et al.*, Proc. Intern. Conf. on Reactions between Complex Nuclei, Nashville 1974 (Ed. R. L. Robinson *et al.*),

Vol. 11. North Holland Publ. Co., Amsterdam (1976), pp. 21–65.
[37]R. K. Gupta, W. Greiner, W. Scheid, Proc. Intern. Summer-School On Nucl. Phys., Predeal, Romania (1974).
[38]H. J. Fink *et al.*, Proc. Intern. Summer-School on Nucl. Phys., Predeal, Romania (1974).
[39]R. K. Gupta, W. Scheid, and W. Greiner, Phys. Rev. Lett. **35**, 353 (1975).
[40]H. Maruhn and W. Greiner, Preprint, Frankfurt (1975).
[41]A. Săndulescu *et al.*, Phys. Lett. B **60**, 225 (1976).
[42]R. K. Gupta *et al.*, Proc. Inter. School-Seminar on Reactions of Heavy Ions with Nuclei and Synthesis of New Elements, Dubna (1975).
[43]R. K. Gupta *et al.*, Proc. Intern. School-Seminar on Reactions of Heavy Ions with Nuclei and Synthesis of New Elements, Dubna (1975).
[44]O. Zohni *et al.*, Z. Phys. A **275**, 235 (1975).
[45]R. K. Gupta and W. Greiner, Proc. Seminar on Electromagnetic Interactions of Nuclei at Low and Medium Energies, Moscow (1975).
[46]R. K. Gupta and W. Greiner, Proc. XIV Intern. Winter Meeting on Nucl. Phys. Bormio, Italy, January 19–23 (1976).
[47]S. Yamaji *et al.*, Preprint, Frankfurt (1976).
[48]J. N. P. Lawrence, Phys. Rev. B **139**, 1227 (1965); Report LA-3774 (1967).
[49]P. T. Ong and W. Scheid, Z. Naturforsch. Teil A **30**, 406 (1975).
[50]W. D. Myers and W. J. Swiatecki, Nucl. Phys. **81**, 1 (1966); Arkiv. Fiz. **36**, 343 (1967).
[51]S. A. E. Johansson, Nucl. Phys. **22**, 529 (1962).
[52]M. Brack, Proc. Intern. Summer-School on Nucl. Phys., Predeal, Romania (1974).
[53]V. M. Strutinskii (Strutinsky) and F. A. Ivanyuk (Ivanjuk), Nucl. Phys. A **255**, 405 (1975).
[54]M. Abramowitz and I. A. Segun, Handbook of Mathematical Functions, Dover, New York (1965).
[55]H. Holm, W. Scheid, and W. Greiner, Phys. Lett. B **29**, 473 (1969); P. W. Riesenfeldt and T. D. Thomas, Phys. Rev. C **2**, 711 (1970); A. S. Jensen and C. Y. Wong, Phys. Rev. C **1**, 1321 (1970).
[56]P. G. Reinhard, Nucl. Phys. A **252**, 133 (1975).
[57]D. R. Inglis, Phys. Rev. **96**, 1059 (1954).
[58]S. T. Belyaev, K. Dan. Vidensk. Selsk. Mat.-Fys. Medd. **31**, No. 11 (1959).
[59]S. Liran *et al.*, Nucl. Phys. A **248**, 191 (1975).
[60]P. Lichtner *et al.*, Phys. Rev. Lett. **28**, 829 (1972).
[61]T. Johansson, S. G. Nilsson, and Z. Symanski, Ann. Phys. (Paris) **5**, 377 (1970).
[62]P. A. Seeger, CERN Report N 70–30, Vol. 1 (1970), p. 217; P. A. Seeger and W. H. Howard, Nucl. Phys. A **238**, 491 (1975).
[63]J. M. Irvine and L. C. Pwu, Preprint, University of Manchester.
[64]L. C. Pwu and B. Castel, Phys. Rev. C **9**, 1650 (1974).
[65]P. Fong, Phys. Rev. C **10**, 1122 (1974); **13**, 1259 (1976).
[66]P. Fong, Phys. Rev. **102**, 434 (1956).
[67]R. W. Hasse, Nucl. Phys. A **128**, 609 (1969); Phys. Rev. C **4**, 572 (1971).
[68]R. Vandenbosch and J. R. Huizenga, Nuclear Fission, Academic Press, New York 1973.
[69]R. Holub, M. G. Mustafa, and H. W. Schmitt, Nucl. Phys. A **222**, 252 (1974).
[70]J. R. Nix and W. J. Swiatecki, Nucl. Phys. **71**, 1 (1965); R. Holub and G. R. Choppin, Nucl. Phys. A **212**, 387 (1973).
[71]U. Facchini and G. Sassi, Contributed Paper at IAEA Consultants Meeting on the Use of Nuclear Theory in Neutron Data Evaluation. Intern. Center for Theoretical Physics, Trieste (Italy), December 8–12, 1975.
[72]B. T. Geilikman and O. V. Zimina, Yad. Fiz. **15**, 457 (1972) [Sov. J. Nucl. Phys. **15**, 256 (1972)].
[73]W. Pauli, in: Handbuch der Physik (Ed. H. Geiger and K. Scheel), Vol. 25 Part 1, Springer, Berlin (1933), p. 120; B. Podolsky, Phys. Rev. **32**, 812 (1928).
[74]K. J. Le Couteur and D. W. Lang, Nucl. Phys. **13**, 32 (1959) (1959).
[75]J. M. Eisenberg and W. Greiner, Microscopic Theory of the Nucleus, North-Holland, Amsterdam (1972) [Russian translation: Atomizdat, Moscow (1976)].
[76]H. Farrar, H. R. Fickel, and R. H. Tomlinson, Canad. J. Phys. **40**, 1017 (1962); H. Farrar and R. H. Tomlinson, Nucl. Phys. **34**, 367 (1962).
[77]A. C. Wahl *et al.*, Phys. Rev. **126**, 1112 (1962).
[78]J. A. McHugh and M. C. Michel, Phys. Rev. **172**, 1160 (1968).
[79]G. Siegert *et al.*, Phys. Rev. Lett. **34**, 1034 (1975).
[80]H. G. Clerc *et al.*, Nucl. Phys. A **247**, 74 (1975); H. G. Clerc *et al.*, Z. Phys. A **274**, 203 (1975).
[81]A. Ghiorso and T. Sikkeland, Phys. Today **20**, No. 9, 25 (1967).
[82]A. Ghiorso *et al.*, Phys. Rev. Lett. **22**, 1317 (1969).
[83]A. Ghiorso *et al.*, Phys. Lett. B **32**, 95 (1970).
[84]A. Ghiorso *et al.*, Phys. Rev. Lett. **24**, 1498 (1970).
[85]A. Ghiorso *et al.*, Phys. Rev. Lett. **33**, 1490 (1974).
[86]G. N. Flerov *et al.*, Phys. Lett. **13**, 73 (1964).
[87]Yu. Ts. Oganessian *et al.*, Nucl. Phys. A **239**, 157 (1975).
[88]G. M. Ter-Akopyan *et al.*, Nucl. Phys. A **255**, 509 (1975).
[89]Yu. Ts. Oganessian *et al.*, Preprint JINR-D7-8099; A. A. Pleve, Proc. Intern. Summer-School on Nucl. Phys., Predeal, Romania. September 1974.
[90]Yu. Ts. Oganessian *et al.*, Nucl. Phys. A **239**, 353 (1975).
[91]H. H. Gutbrod, W. G. Winn, and M. Blann, Phys. Rev. Lett. **30**, 1259 (1973).
[92]J. M. Nitschke, Private Communication to Prof. W. Greiner.
[93]R. Bengtsson *et al.*, Phys. Lett. B **55**, 6 (1975).
[94]M. G. Mustafa and K. Kumar, Phys. Rev. C **12**, 1638 (1975).
[95]J. V. Kratz, A. E. Norris, and G. T. Seaborg, Phys. Rev. Lett. **33**, 502 (1974).
[96]R. J. Otto *et al.*, Phys. Rev. Lett. **36**, 135 (1976).
[97]F. Hanappe *et al.*, Phys. Rev. Lett. **32**, 738 (1974).
[98]K. L. Wolf *et al.*, Phys. Rev. Lett. **33**, 1105 (1974).
[99]J. Péter, C. Ngô, and B. Tamain, J. Phys. Lett. **36**, 23 (1975); Nucl. Phys. A **250**, 351 (1975).
[100]H. C. Britt *et al.*, Los. Alamos Report LA-UR-75-2072.
[101]W. U. Schröeder *et al.*, Phys. Rev. Lett. **36**, 514 (1976).
[102]P. A. Cherdantsev, I. P. Chernov, and G. A. Vershinin, Phys. Lett. B **55**, 137 (1975).
[103]W. Scheid and W. Greiner, Z. Phys. **226**, 364 (1969); H. J. Krappe and J. R. Nix, Contribution to the Third Symposium on the Phys. and Chem. of Fission, Rochester, New York (1973).
[104]E. D. Mshelia, W. Scheid, and W. Greiner, Nuovo Cimento **30**, 589 (1975) and the references therein.
[105]P. Bergmann and H. J. Scheefer, Z. Naturforsch., Teil A **29**, 1003 (1974).
[106]J. Hahn, Diploma Thesis, Institute for Theoretical Physics, University of Frankfurt am Main.
[107]H. J. Lustig, Diploma Thesis, Institute for Theoretical Physics, University of Frankfurt am Main.

Translated by Julian B. Barbour